



---

Year: 2019

---

## A 34 is a BACE1-derived degradation intermediate associated with amyloid clearance and Alzheimer's disease progression

Liebsch, Filip; Kulic, Luka; Teunissen, Charlotte; Shobo, Adeola; Ulku, Irem; Engelschalt, Vivienne; Hancock, Mark A; van der Flier, Wiesje M; Kunach, Peter; Rosa-Neto, Pedro; Scheltens, Philip; Poirier, Judes; Saftig, Paul; Bateman, Randall J; Breitner, John; Hock, Christoph; Multhaup, Gerhard

**Abstract:** The beta-site APP cleaving enzyme 1 (BACE1) is known primarily for its initial cleavage of the amyloid precursor protein (APP), which ultimately leads to the generation of A peptides. Here, we provide evidence that altered BACE1 levels and activity impact the degradation of A 40 and A 42 into a common A 34 intermediate. Using human cerebrospinal fluid (CSF) samples from the Amsterdam Dementia Cohort, we show that A 34 is elevated in individuals with mild cognitive impairment who later progressed to dementia. Furthermore, A 34 levels correlate with the overall A clearance rates in amyloid positive individuals. Using CSF samples from the PREVENT-AD cohort (cognitively normal individuals at risk for Alzheimer's disease), we further demonstrate that the A 34/A 42 ratio, representing A degradation and cortical deposition, associates with pre-clinical markers of neurodegeneration. We propose that A 34 represents a marker of amyloid clearance and may be helpful for the characterization of A turnover in clinical samples.

DOI: <https://doi.org/10.1038/s41467-019-10152-w>

Posted at the Zurich Open Repository and Archive, University of Zurich

ZORA URL: <https://doi.org/10.5167/uzh-172098>

Journal Article

Published Version



The following work is licensed under a Creative Commons: Attribution 4.0 International (CC BY 4.0) License.

Originally published at:

Liebsch, Filip; Kulic, Luka; Teunissen, Charlotte; Shobo, Adeola; Ulku, Irem; Engelschalt, Vivienne; Hancock, Mark A; van der Flier, Wiesje M; Kunach, Peter; Rosa-Neto, Pedro; Scheltens, Philip; Poirier, Judes; Saftig, Paul; Bateman, Randall J; Breitner, John; Hock, Christoph; Multhaup, Gerhard (2019). A 34 is a BACE1-derived degradation intermediate associated with amyloid clearance and Alzheimer's disease progression. *Nature Communications*, 10(1):2240.

DOI: <https://doi.org/10.1038/s41467-019-10152-w>

ARTICLE

<https://doi.org/10.1038/s41467-019-10152-w>

OPEN

# A $\beta$ 34 is a BACE1-derived degradation intermediate associated with amyloid clearance and Alzheimer's disease progression

Filip Liebsch<sup>1</sup>, Luka Kulic<sup>2</sup>, Charlotte Teunissen<sup>3</sup>, Adeola Shobo<sup>1</sup>, Irem Ulku<sup>1</sup>, Vivienne Engelschalt<sup>4</sup>, Mark A. Hancock<sup>5</sup>, Wiesje M. van der Flier<sup>6</sup>, Peter Kunach<sup>7</sup>, Pedro Rosa-Neto<sup>7</sup>, Philip Scheltens<sup>6</sup>, Judes Poirier<sup>8</sup>, Paul Saftig<sup>9</sup>, Randall J. Bateman<sup>10</sup>, John Breitner<sup>8</sup>, Christoph Hock<sup>2,11</sup> & Gerhard Multhaup<sup>1</sup>

The beta-site APP cleaving enzyme 1 (BACE1) is known primarily for its initial cleavage of the amyloid precursor protein (APP), which ultimately leads to the generation of A $\beta$  peptides. Here, we provide evidence that altered BACE1 levels and activity impact the degradation of A $\beta$ 40 and A $\beta$ 42 into a common A $\beta$ 34 intermediate. Using human cerebrospinal fluid (CSF) samples from the Amsterdam Dementia Cohort, we show that A $\beta$ 34 is elevated in individuals with mild cognitive impairment who later progressed to dementia. Furthermore, A $\beta$ 34 levels correlate with the overall A $\beta$  clearance rates in amyloid positive individuals. Using CSF samples from the PREVENT-AD cohort (cognitively normal individuals at risk for Alzheimer's disease), we further demonstrate that the A $\beta$ 34/A $\beta$ 42 ratio, representing A $\beta$  degradation and cortical deposition, associates with pre-clinical markers of neurodegeneration. We propose that A $\beta$ 34 represents a marker of amyloid clearance and may be helpful for the characterization of A $\beta$  turnover in clinical samples.

<sup>1</sup> Department of Pharmacology and Therapeutics and Integrated Program in Neuroscience, McGill University, Montreal, QC H3G 1Y6, Canada. <sup>2</sup> Institute for Regenerative Medicine, University of Zurich, CH-8952 Schlieren, Switzerland. <sup>3</sup> Department of Clinical Chemistry, Amsterdam Neuroscience, Amsterdam UMC, Vrije Universiteit Amsterdam, 1081HZ Amsterdam, The Netherlands. <sup>4</sup> Institut für Chemie und Biochemie, Freie Universität Berlin, 14195 Berlin, Germany. <sup>5</sup> SPR-MS Facility, McGill University, Montreal, QC H3G 1Y6, Canada. <sup>6</sup> Alzheimer Center Amsterdam, Department of Neurology, Amsterdam Neuroscience, Amsterdam UMC, Vrije Universiteit Amsterdam, Amsterdam 1081HZ, The Netherlands. <sup>7</sup> Translational Neuroimaging Laboratory, The McGill University Research Centre for Studies in Aging, Alzheimer's Disease Research Unit, Douglas Research Institute, McGill University, Montreal H4H 1R3 QC, Canada. <sup>8</sup> Department of Psychiatry, McGill University, Montreal, QC H4H 1R3, Canada. <sup>9</sup> Biochemisches Institut, Christian-Albrechts-Universität-Kiel, 24118 Kiel, Germany. <sup>10</sup> Department of Neurology, Washington University in St. Louis, St. Louis, MO 63110, USA. <sup>11</sup> Neurimmune, CH-8952 Schlieren, Switzerland. Correspondence and requests for materials should be addressed to G.M. (email: [gerhard.multhaup@mcgill.ca](mailto:gerhard.multhaup@mcgill.ca))

The pathogenesis of Alzheimer's disease (AD) is characterized by amyloid- $\beta$  ( $A\beta$ ) plaque formation in the brain<sup>1,2</sup>. Sequential cleavage of the amyloid precursor protein (APP) by  $\beta$ -secretase (BACE1) and the  $\gamma$ -secretase complex results in the generation of  $A\beta$  species of varying lengths, e.g.,  $A\beta$ 38,  $A\beta$ 40, and  $A\beta$ 42<sup>3,4,5,6</sup>. More neurotoxic than  $A\beta$ 38 or  $A\beta$ 40, the  $A\beta$ 42 peptide is prone to form oligomers (i.e., precursor to larger fibrils), which are thought to contribute to plaque formation and cognitive decline<sup>7</sup>.

To block the first step of amyloid production, the pharmaceutical industry has focused on inhibitors of BACE1 as a therapeutic strategy for AD. However, BACE1 inhibitors have failed in clinical trials due to side effects, possible toxicity, or the absence of beneficial cognitive outcomes<sup>8</sup>. The lack of success may also relate to the timing of administration, since treatments in the symptomatic stage might be too late.

BACE1 levels are elevated in the neocortex of AD patients<sup>9–11</sup>. Perhaps as a pathological response to fibrillar  $A\beta$ , the accumulation of BACE1 in the vicinity of amyloid plaques can enhance local  $A\beta$  generation<sup>12–16</sup>. However, excess BACE1 activity can also lead to (i) alternative APP processing at the  $\beta'$ -site, generating metabolically labile  $A\beta$ 11-X peptides<sup>17</sup>, or (ii)  $A\beta$  degradation, by catalyzing the C-terminal truncation of  $A\beta$ 40 and  $A\beta$ 42 into non-amyloidogenic  $A\beta$ 34<sup>18–21</sup>. In human and canine *in vivo* studies, cerebrospinal fluid (CSF) levels of  $A\beta$ 34 decline with pharmacological BACE1 inhibition, most likely due to an interruption of the BACE1-mediated degradation of  $A\beta$ 40 and  $A\beta$ 42<sup>22,23</sup>. However, the amyloidolytic roles of BACE1 in  $A\beta$  metabolism are currently not well defined, either in health (i.e., physiological homeostasis) or disease (i.e., AD pathogenesis).

The pathological cascade of sporadic AD appears to be triggered by impaired  $A\beta$  degradation and clearance<sup>24</sup>.  $A\beta$  clearance from the brain can occur by several mechanisms including interstitial fluid drainage, cellular uptake, and passive elimination<sup>25,26</sup>. Enzymatic degradation generates specific patterns of soluble  $A\beta$  peptides in the CSF<sup>27</sup>, as mediated by  $A\beta$ -degrading enzymes (ADEs), which include metalloprotease family members such as endothelin-converting enzyme (ECE), insulin-degrading enzyme (IDE), and neprilysin (NEP)<sup>28</sup>. Results obtained with <sup>18</sup>O-labeling mass spectrometry demonstrated that the  $A\beta$  peptide pattern in CSF is not generated by proteolytic activities in CSF itself—except in the acute phase of a bacterial meningitis<sup>29</sup>—but  $A\beta$  fragments are likely generated prior to entering the CSF.

The normal clearance rate for  $A\beta$ 40 or  $A\beta$ 42 in human CSF is estimated to be ~8% per hour<sup>30</sup>, but clearance is impaired by approximately 30% in AD patients<sup>24</sup>.  $A\beta$  stable isotope labeling kinetics (SILK) studies found that production and clearance of soluble  $A\beta$  isoforms are similar for  $A\beta$ 38 and  $A\beta$ 40, but  $A\beta$ 42 turnover is altered with increasing age and amyloidosis<sup>31</sup>.

Since we have previously shown that  $A\beta$ 34 is a common intermediate in the enzymatic processing of two distinct  $A\beta$  degradation pathways<sup>6</sup>, the present study examines the levels and metabolism of  $A\beta$ 34 in the brains of BACE1-deficient mice, in brain and CSF of rats treated with a BACE1-specific inhibitor, a cultured human neuronal cell line (SH-SY5Y), and CSF samples from individuals at various clinical stages of AD. To accomplish this, we utilize a custom, ultra-sensitive Meso Scale Discovery (MSD) electrochemiluminescence assay, using a monoclonal neopeptide antibody that binds specifically to the C-terminus of  $A\beta$ 34 with nanomolar affinity. Our results show that cerebral BACE1 levels are limiting for  $A\beta$ 34 generation *in vivo*. Specifically, in well-characterized clinical groups, CSF levels of  $A\beta$ 34 are notably elevated in individuals with mild cognitive impairment (MCI) who later progressed to AD dementia. Compared with the classical  $A\beta$ 40/ $A\beta$ 42 ratio (i.e., marker of amyloid deposition in

clinical practice), the  $A\beta$ 34/ $A\beta$ 42 ratio improves our ability to distinguish between individuals with MCI who later converted to AD from those who did not. Among cognitively normal individuals at risk for AD, an elevated CSF- $A\beta$ 34/ $A\beta$ 42 ratio is detected together with current biomarkers of pre-clinical AD, such as elevated CSF levels of total-tau (t-tau) and phosphorylated ( $P_{181}$ )-tau. Furthermore, the overall  $A\beta$  clearance rates positively correlate with CSF- $A\beta$ 34 levels in amyloid-positive ( $A\beta$ +) individuals.

While the interesting  $A\beta$ 34 biology of this article directly impacts the design of future studies looking at  $A\beta$  turnover and clinical studies involving BACE inhibitors, we anticipate that combining markers of amyloid clearance ( $A\beta$ 34 measurements) and deposition (well-established  $A\beta$ 42 measurements in CSF) may provide a more complete biomarker panel to assess AD samples (i.e., early-stage biochemical changes vs. late-stage plaque/tangle pathology). Future studies are needed to validate whether an increased CSF- $A\beta$ 34/ $A\beta$ 42 ratio may provide an opportunity for earlier intervention strategies.

## Results

**Cerebral  $A\beta$ 34 is decreased in BACE1-deficient mice.** Given that BACE1 can directly cleave longer  $A\beta$  species between Leu34 and Met35 *in vitro*<sup>19,20</sup> (Supplementary Fig. 1), we hypothesized that  $A\beta$  degradation would be affected by altered BACE1 expression levels *in vivo*. To test this, we analyzed endogenous cerebral BACE1, APP, and  $A\beta$  levels from BACE1<sup>-/-</sup> and BACE1<sup>+/-</sup> mice, as well as their wild-type (BACE1<sup>+/+</sup>) littermates (Fig. 1a–g). In agreement with previously published results<sup>32,33</sup>, BACE1 protein levels in the brain of BACE1<sup>+/-</sup> mice were approximately half that of wild-type mice, as analyzed by western blot (Fig. 1a, b). Furthermore, BACE1<sup>-/-</sup> mice had significantly elevated levels of cerebral APP and/or soluble APP (sAPP) compared with their BACE1<sup>+/-</sup> and wild-type littermates, whereas there was no significant difference between BACE1<sup>+/-</sup> and wild-type animals (Fig. 1a, c). Notably, the former is possibly due to increased levels of full-length APP<sup>34</sup>.

We next measured endogenous levels of  $A\beta$ 34,  $A\beta$ 38,  $A\beta$ 40, and  $A\beta$ 42 peptides in the brains of these same mice using a custom 4-plex MSD multiplexing assay (Supplementary Methods, Supplementary Figs. 2, 3). In agreement with previous findings in mice and rats<sup>32,35,36</sup>,  $A\beta$ 38,  $A\beta$ 40, and  $A\beta$ 42 were significantly decreased in BACE1<sup>-/-</sup> mouse brains, whereas their levels did not differ significantly between BACE1<sup>+/-</sup> and wild-type littermates (Fig. 1e–g). As expected for a fragment generated by BACE1 activity, cerebral  $A\beta$ 34 levels were decreased in BACE1<sup>-/-</sup> mice compared with BACE1<sup>+/-</sup> (Fig. 1d). Notably,  $A\beta$ 34 levels were also significantly lower in BACE1<sup>+/-</sup> mice compared with wild-type littermates. Apparently, the cerebral amyloidogenic processing of endogenous APP by BACE1 is not impaired by a 50% decreased enzyme availability, as it is indistinguishable in heterozygous knockouts and wild-type littermates (Fig. 1e–g). Furthermore, the  $A\beta$ 34/ $A\beta$ 38,  $A\beta$ 34/ $A\beta$ 40, and  $A\beta$ 34/ $A\beta$ 42 ratios revealed a step-wise decrease with decreasing BACE1 levels (Fig. 1h–j). These findings support the concept that cerebral BACE1 levels are limiting for its amyloidolytic activity *in vivo* relying on conversion of the longer  $A\beta$  species to  $A\beta$ 34, whereas BACE1 levels are not limiting for APP cleavage resulting in  $A\beta$ 38,  $A\beta$ 40, and  $A\beta$ 42.

**BACE1 inhibition lowers rat CSF and brain  $A\beta$ 34 levels.** To independently assess whether the above findings hold true for the pharmacological intervention with BACE1 activity, wild-type rats were treated with the BACE1-specific inhibitor MK-8931<sup>37</sup>. The inhibitor had no effect on cerebral APP and/or sAPP levels

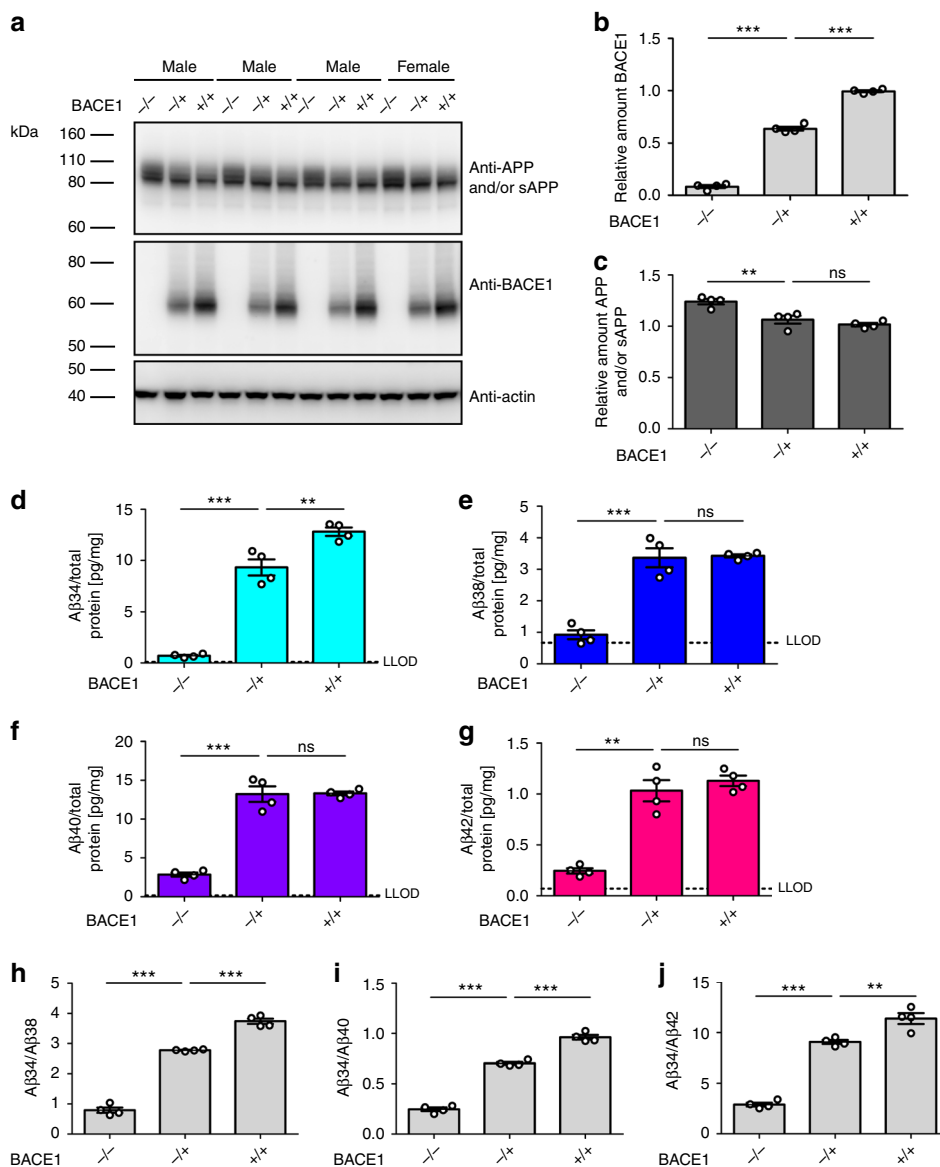


**Fig. 1** Endogenous BACE1 generates Aβ34 in the murine brain. Endogenous levels of murine APP and/or sAPP, BACE1, and Aβ in BACE1<sup>-/-</sup>, BACE1<sup>+/-</sup>, and wild-type littermates (+/+). *N* = 4 animals per group. Western blot of endogenous APP and/or sAPP and BACE1 expression in male and female mice (**a**) and corresponding quantification of relative protein amounts of BACE1 (**b**) and APP and/or sAPP (**c**). Quantification (pg/mg total protein) of absolute amounts of Aβ34 (**d**), Aβ38 (**e**), Aβ40 (**f**), and Aβ42 (**g**) as determined by custom 4-plex MSD multiplexing assays. Ratios of Aβ34/Aβ38 (**h**), Aβ34/Aβ40 (**i**), and Aβ34/Aβ42 (**j**) are displayed. Statistics: **b** one-way ANOVA,  $F(2, 9) = 1021, p < 0.0001$ , **c** one-way ANOVA,  $F(2, 9) = 17.28, p < 0.001$ , **d** one-way ANOVA,  $F(2, 9) = 145.7, p < 0.0001$ , **e** one-way ANOVA,  $F(2, 9) = 53.68, p < 0.0001$ , **f** one-way ANOVA,  $F(2, 9) = 95.65, p < 0.0001$ , **g** one-way ANOVA,  $F(2, 9) = 49.70, p < 0.0001$ , **h** one-way ANOVA,  $F(2, 9) = 425.2, p < 0.0001$ , **i** one-way ANOVA,  $F(2, 9) = 378.0, p < 0.0001$ , **j** one-way ANOVA,  $F(2, 9) = 157.6, p < 0.0001$ . Bars and error bars indicate mean  $\pm$  s.e.m. Tukey's post-hoc tests were performed for pairwise comparisons; selected comparisons are highlighted \*\*\* $p < 0.001$ , \*\* $p < 0.01$ , ns = nonsignificant  $p > 0.05$ . For each target, the MSD software computes the lower limit of detection (LLOD) as 2.5 standard deviations above the blank

(Fig. 2a, b). Cerebral Aβ34 levels were significantly decreased in rats treated with concentrations of 1 and 20 mg/kg (Fig. 2c). In contrast, cerebral Aβ40 and Aβ42 levels were only decreased in the 20 mg/kg but not the 1 mg/kg cohort (Fig. 2d, e). Consequently, the ratios Aβ34/Aβ40 and Aβ34/Aβ42 were significantly decreased at 1 and 20 mg/kg (Fig. 2f, g). In agreement with our findings in BACE1<sup>+/-</sup> mice, these results indicate that cerebral Aβ34 levels are more sensitive to changes in BACE1 activity than the longer Aβ species.

We next measured CSF levels of Aβ34, Aβ38, Aβ40, and Aβ42. CSF-Aβ34 was significantly decreased in the cohorts treated with 1 and 20 mg/kg (Fig. 2h), however, there was no change for Aβ38,

Aβ40, and Aβ42 (Fig. 2i–k). Furthermore, the ratios Aβ34/Aβ38, Aβ34/Aβ40, and Aβ34/Aβ42 in CSF were significantly decreased in the animals treated with 1 and 20 mg/kg (Fig. 2l–n). Overall, the results of these experiments demonstrate that the pharmacological inhibition of BACE1 differentially affects the amyloidogenic and the amyloidolytic activities of the enzyme in vivo. Importantly, the latter seems more sensitive than the former to the amount (Fig. 1) and activity (Fig. 2) of BACE1.

**Aβ34 is an Aβ degradation intermediate.** Previous studies showed that APP and BACE1 expression can change the quantity

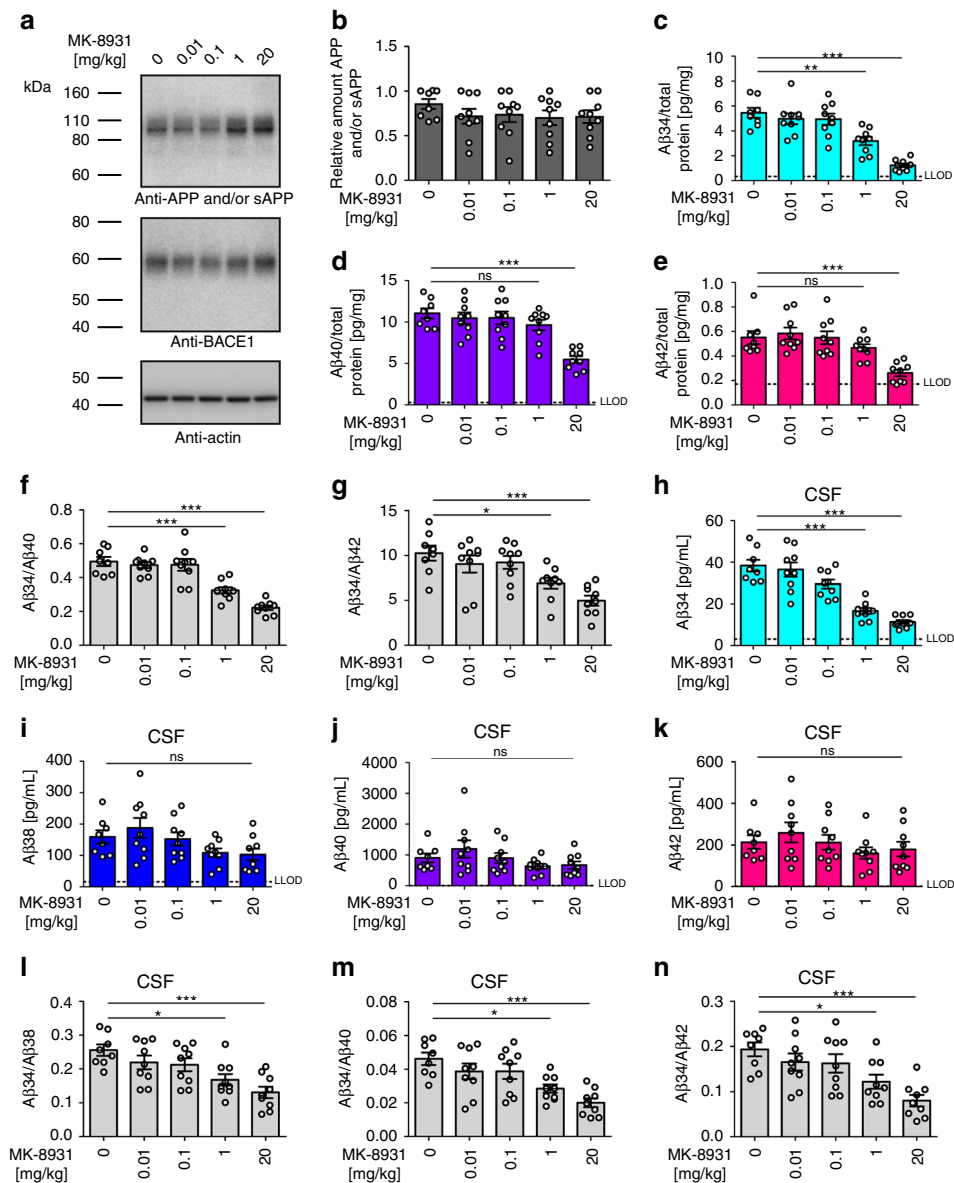


**Fig. 2** Pharmacological inhibition of A $\beta$ 34 generation in rats. Endogenous levels of APP and/or sAPP, BACE1, and A $\beta$  in rats 1 h after intravenous injection of the indicated concentrations (mg/kg) of the BACE1-specific inhibitor (MK-8931)  $n = 9$  animals per group or vehicle  $n = 8$  animals. Western blot of endogenous APP and/or sAPP and BACE1 expression (**a**) and corresponding quantification of relative protein amounts of APP and/or sAPP (**b**). Quantification (pg/mg total protein) of absolute amounts of A $\beta$ 34 (**c**), A $\beta$ 40 (**d**), and A $\beta$ 42 (**e**) as determined by custom MSD multiplexing assays. Ratios of A $\beta$ 34/A $\beta$ 40 (**f**) and A $\beta$ 34/A $\beta$ 2 (**g**) are displayed. Quantification of CSF levels of A $\beta$ 34 (**h**), A $\beta$ 38 (**i**), A $\beta$ 40 (**j**), and A $\beta$ 42 (**k**), as well as display of the ratios A $\beta$ 34/A $\beta$ 38 (**l**), A $\beta$ 34/A $\beta$ 40 (**m**), and A $\beta$ 34/A $\beta$ 42 (**n**). Statistics: **b** one-way ANOVA,  $F(4, 39) = 0.63$ ,  $p > 0.05$ , **c** one-way ANOVA,  $F(4, 39) = 22.40$ ,  $p < 0.0001$ , **d** one-way ANOVA,  $F(4, 39) = 12.81$ ,  $p < 0.0001$ , **e** one-way ANOVA,  $F(4, 39) = 9.38$ ,  $p < 0.0001$ , **f** one-way ANOVA,  $F(4, 39) = 25.93$ ,  $p < 0.0001$ , **g** one-way ANOVA,  $F(4, 39) = 8.02$ ,  $p < 0.0001$ , **h** one-way ANOVA,  $F(4, 39) = 26.55$ ,  $p < 0.0001$ , **i** one-way ANOVA,  $F(4, 39) = 2.69$ ,  $p < 0.05$ , **j** one-way ANOVA,  $F(4, 39) = 1.71$ ,  $p > 0.05$ , **k** one-way ANOVA,  $F(4, 39) = 1.09$ ,  $p > 0.05$ , **l** one-way ANOVA,  $F(4, 39) = 6.87$ ,  $p < 0.001$ , **m** one-way ANOVA,  $F(4, 39) = 7.36$ ,  $p < 0.001$ , **n** one-way ANOVA,  $F(4, 39) = 6.74$ ,  $p < 0.001$ . Bars and error bars indicate mean  $\pm$  s.e.m. Tukey's post-hoc tests were performed for pairwise comparisons; selected comparisons are highlighted \*\*\* $p < 0.001$ , \*\* $p < 0.01$ , \* $p < 0.05$ , ns = nonsignificant  $p > 0.05$

of A $\beta$  produced<sup>33,38</sup>. Therefore, we tested whether A $\beta$ 34 levels would be affected by a surplus of either substrate or enzyme in a human neuronal cell type. Using human neuroblastoma (SH-SY5Y) cells stably overexpressing APP or BACE1 (Fig. 3a), we measured secreted levels of A $\beta$ 34, A $\beta$ 38, A $\beta$ 40, and A $\beta$ 42 in the supernatants using the ultra-sensitive 4-plex assay, whereas sAPP $\beta$  and sAPP<sub>total</sub> were detected by western blot (Fig. 3a–h). Overexpression of APP mildly increased A $\beta$ 34 levels (not statistically different from empty plasmid (Mock)-transfected cells,  $p = 0.06$ ) and significantly elevated sAPP $\beta$ , sAPP<sub>total</sub>, A $\beta$ 38, A $\beta$ 40, and A $\beta$ 42, as compared with Mock-transfected cells (Fig. 3b–h).

Conversely, in BACE1-overexpressing cells, A $\beta$ 34 levels were significantly elevated approximately threefold compared with APP-overexpressing conditions, whereas A $\beta$ 38, A $\beta$ 40, and A $\beta$ 42 levels showed only a mild trend toward elevation compared with the control (Fig. 3e–h). Furthermore, more APP was shed from either of these cell lines (Fig. 3c, d). Note that the apparent molecular weights of endogenous APP and sAPPs are slightly higher than those from APP695-transfected cells (Fig. 3a, b), which is likely due to the fact that undifferentiated SH-SY5Y cells express not only APP695 but also splice variants with KPI- and OX-2 domains<sup>39,40</sup>. Overall, we conclude that a surplus of either



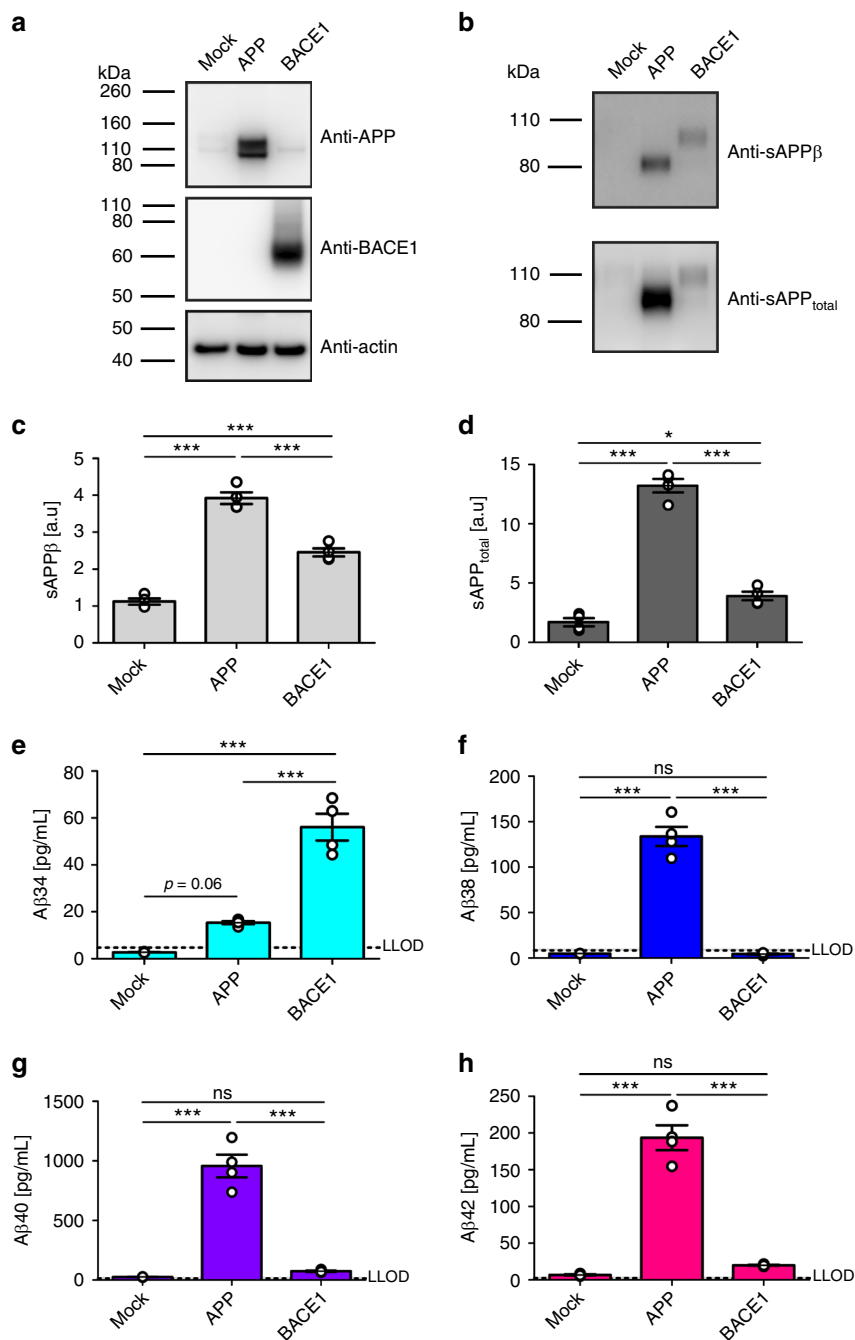


**Fig. 3** Surplus of APP or BACE1 differentially affect APP processing. Using SH-SY5Y cells stably expressing APP695 or BACE1, cleavage of APP was analyzed by western blot and ultra-sensitive MSD assay. Representative western blots for the examination of APP, BACE1, sAPP $\beta$ , and sAPP $_{total}$  (**a, b**), and the corresponding quantification for the relative amounts of sAPP $\beta$  (**c**) and sAPP $_{total}$  (**d**). MSD multiplexing to quantify the absolute amounts of A $\beta$ 34 (**e**), A $\beta$ 38 (**f**), A $\beta$ 40 (**g**), and A $\beta$ 42 (**h**). Data were collected from four independent experiments. Bars and error bars indicate mean  $\pm$  s.e.m. **c-h** Data were analyzed with one-way ANOVAs and Tukey's post-hoc tests were performed for pairwise comparisons; selected comparisons are highlighted \*\*\* $p < 0.001$ , \* $p < 0.05$ , ns = nonsignificant  $p > 0.05$ . **c** sAPP $\beta$ ,  $F(2, 9) = 131.2$ ,  $p < 0.0001$ , **d** sAPP $_{total}$ ,  $F(2, 9) = 190.3$ ,  $p < 0.0001$ , **e** A $\beta$ 34,  $F(2, 9) = 70.04$ ,  $p < 0.0001$ , **f** A $\beta$ 38,  $F(2, 9) = 149.0$ ,  $p < 0.0001$ , **g** A $\beta$ 40,  $F(2, 9) = 89.96$ ,  $p < 0.0001$ , **h** A $\beta$ 42,  $F(2, 9) = 113.6$ ,  $p < 0.0001$

substrate or enzyme affects APP processing differentially in the human neuronal cell line, resulting in (i) increased A $\beta$ 38, A $\beta$ 40, and A $\beta$ 42 release from APP-overexpressing cells, or (ii) an enhanced degradation of all longer A $\beta$  forms into A $\beta$ 34 in BACE1-overexpressing cells.

To investigate whether BACE1 inhibition differentially affects the A $\beta$  profiles, SH-SY5Y cells overexpressing APP or BACE1 were treated with MK-8931<sup>37</sup> at approximately 20-fold of its published IC<sub>50</sub> (i.e., [MK-8931] = 100 nM, Fig. 4, Supplementary

Fig. 4). Conditioned medium from APP-overexpressing SH-SY5Y cells showed significantly decreased levels of sAPP $\beta$ , A $\beta$ 34, A $\beta$ 38, A $\beta$ 40, and A $\beta$ 42 in the presence of MK-8931 (Fig. 4a-d, Supplementary Fig. 4a-c). Furthermore, a dose-inhibition curve for MK-8931 was performed and sAPP $\beta$  (western blot), A $\beta$ 34 (MSD 1-plex), and A $\beta$ 40 (MSD 1-plex) were measured (Supplementary Fig. 4d-f). In APP-overexpressing SH-SY5Y cells, MK-8931 dose-dependently decreased sAPP $\beta$  ( $pIC_{50} = 10.7 \pm 0.3$  (s.e.m.)), A $\beta$ 34 ( $pIC_{50} = 14.1 \pm 0.6$ ), and A $\beta$ 40 levels

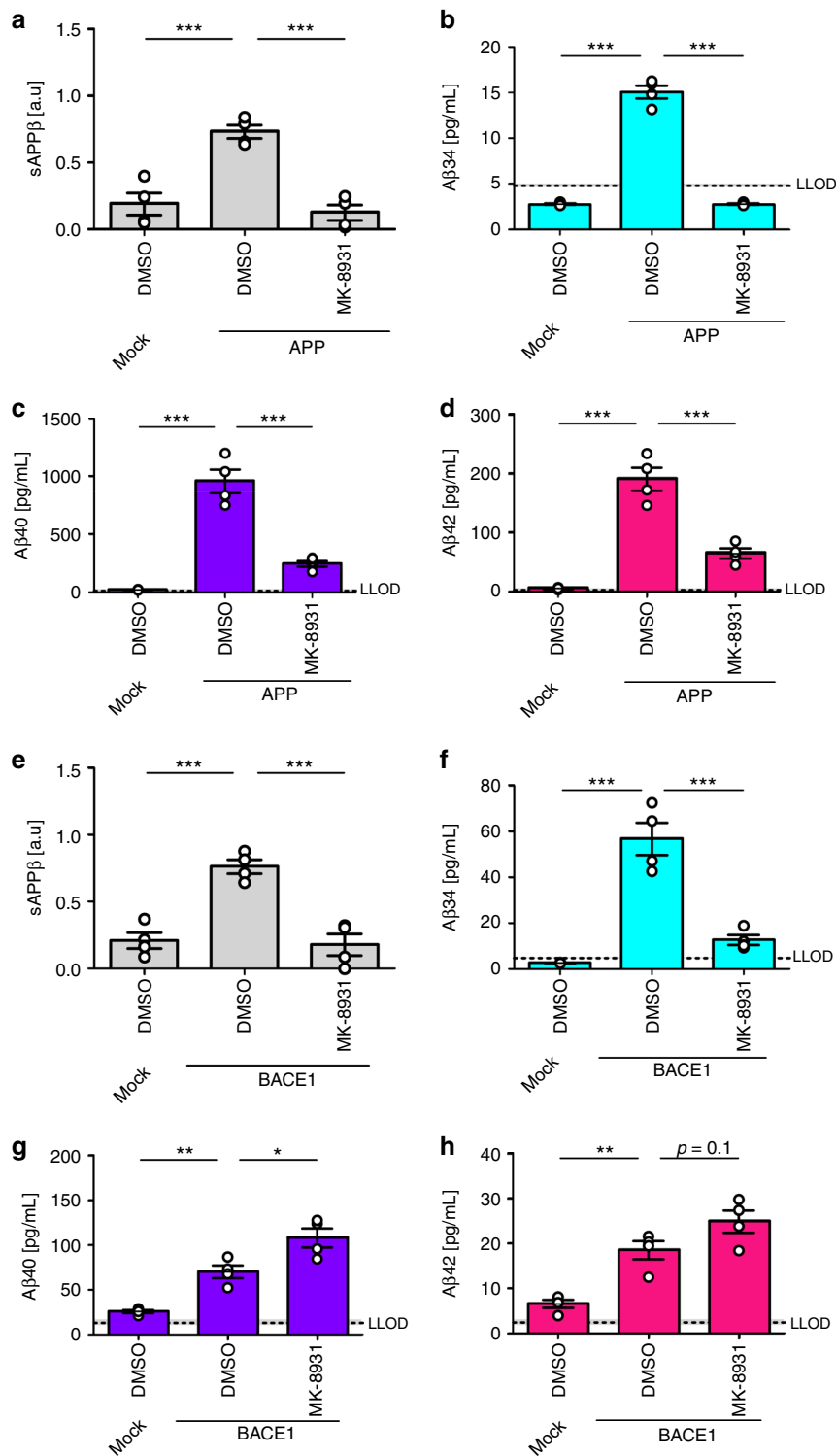


**Fig. 4** Surplus of APP or BACE1 affect BACE1 inhibition. Cleavage of APP was analyzed by western blot and ultra-sensitive MSD assays. Absolute or relative amounts of products were quantified from SH-SY5Y cells stably expressing APP695 (**a-d**) or BACE1 (**e-h**). Quantification of relative amounts of sAPPβ (**a, e**), and absolute amounts of Aβ34 (**b, f**), Aβ40 (**c, g**), and Aβ42 (**d, h**). Data were collected from four independent experiments. Bars and error bars indicate mean ± s.e.m. Tukey's post-hoc tests were performed for pairwise comparisons; selected comparisons are highlighted \*\*\* $p < 0.001$ , \*\* $p < 0.01$ , \* $p < 0.05$ . **a** sAPPβ, one-way ANOVA,  $F(2, 9) = 26.6$ ,  $p < 0.001$ , **b** Aβ34, one-way ANOVA,  $F(2, 9) = 296.1$ ,  $p < 0.0001$ , **c** Aβ40, one-way ANOVA,  $F(2, 9) = 65.9$ ,  $p < 0.0001$ , **d** Aβ42, one-way ANOVA,  $F(2, 9) = 59.4$ ,  $p < 0.0001$ , **e** sAPPβ, one-way ANOVA,  $F(2, 9) = 25.4$ ,  $p < 0.001$ , **f** Aβ34, one-way ANOVA,  $F(2, 9) = 45.3$ ,  $p < 0.0001$ , **g** Aβ40, one-way ANOVA,  $F(2, 9) = 30.8$ ,  $p < 0.0001$ , **h** Aβ42, one-way ANOVA,  $F(2, 9) = 23.3$ ,  $p < 0.001$

( $pIC_{50} = 11.3 \pm 0.7$ ) (Supplementary Fig. 4d–f). In contrast, in conditioned medium from BACE1-overexpressing SH-SY5Y cells, only the levels of sAPP $\beta$  and A $\beta$ 34 were significantly decreased in the presence of the inhibitor (Fig. 4e, f, Supplementary Fig. 4g, h), whereas A $\beta$ 38 and A $\beta$ 40 were significantly increased and A $\beta$ 42 levels showed a trend for being elevated,  $p = 0.1$  (Supplementary Fig. 4i, Fig. 4g, h). In BACE1-overexpressing SH-SY5Y cells, MK-8931 only dose-dependently decreased sAPP $\beta$  ( $pIC_{50} = 8.3 \pm 0.3$ ) and A $\beta$ 34 levels ( $pIC_{50} = 7.3 \pm 0.2$ ) (Supplementary Fig. 4j, l). Interestingly, A $\beta$ 40 levels were decreased at high inhibitor concentrations ( $p[MK-8931] > -6$ ), elevated at intermediate concentrations ( $-10 < p[MK-8931] < -6$ ) and unchanged at low concentrations ( $-10 > p[MK-8931]$ ) (Supplementary Fig. 4k). Ultimately, these results show that the response to pharmacological BACE1 inhibition depends on the relative abundances of BACE1 and its substrate APP. Notably, inhibition with insufficient amounts of compound at high levels of BACE1 could result in undesired elevated A $\beta$ 40 and A $\beta$ 42 levels. However, BACE1 inhibitor doses used in vivo can effectively reduce the levels of longer A $\beta$  species<sup>37</sup>.

ADEs include the metalloproteases, a large group of proteases that likely cleave A $\beta$  peptide substrates<sup>28</sup>. In general, ADE-derived fragments are short, soluble, and not prone to aggregate. To investigate how A $\beta$ 34, A $\beta$ 38, A $\beta$ 40, and A $\beta$ 42 degradation is affected by metalloproteases, we treated APP- or BACE1-overexpressing SH-SY5Y cells with the metalloprotease inhibitor phosphoramidon (PA). Supernatants were analyzed using the 4-plex MSD assay as before (Fig. 5). In APP-overexpressing cells, PA treatment significantly elevated the levels of all A $\beta$  species measured (Fig. 5a–d). In the presence of PA, however, A $\beta$ 34 was increased approximately ninefold, whereas the levels of A $\beta$ 38, A $\beta$ 40, and A $\beta$ 42 were only about two to threefold higher (Fig. 5a–d). In agreement with previously published data<sup>21</sup>, these findings imply that A $\beta$ 34 is more sensitive to metalloprotease-mediated degradation compared with the longer species tested. In BACE1-overexpressing cells, A $\beta$ 34 levels were increased by about 2.5-fold in the presence of PA, whereas A $\beta$ 38, A $\beta$ 40, and A $\beta$ 42 levels were not significantly changed (Fig. 5a–d). Together, these results suggest that A $\beta$ 34 is a stable A $\beta$  degradation intermediate of the amyloid degradation cascade. Thus, we propose that in the presence of surplus APP substrate, A $\beta$ 38, A $\beta$ 40, and A $\beta$ 42 are degraded by both metalloproteases and the BACE1-mediated A $\beta$ 34 pathway (Fig. 5e). Conversely, in the presence of surplus BACE1 enzyme, longer forms of A $\beta$  are predominantly degraded by BACE1, yielding A $\beta$ 34 as a metastable cleavage product (Fig. 5e).

**CSF-A $\beta$ 34 levels are associated with AD progression.** To explore the associations between A $\beta$ 34 and putative changes in BACE1 expression observed in AD<sup>9–11</sup>, we analyzed A $\beta$ 34 in 98 human CSF samples from the Amsterdam Dementia Cohort. Samples were collected from 22 people with subjective cognitive complaints (SC), 17 with MCI that remained stable, 27 with MCI that later progressed to AD dementia (i.e., MCI converters), and 32 AD patients. Using our MSD assay, we found significantly elevated A $\beta$ 34 levels in the CSF of MCI converters when compared with SC or MCI stable (Fig. 6a). Furthermore, the levels in MCI converters showed a trend for being elevated compared with AD patients (the greater variability is likely due to a larger heterogeneity in this group). CSF-A $\beta$ 34 levels from all groups did not associate with age, the genetic risk allele *APOE*  $\epsilon$ 4, or gender (Supplementary Fig. 5a–c). As expected, there was a decrease in A $\beta$ 42 in AD patients and MCI converters compared with the SC and MCI stable group (Fig. 6b). These changes are likely due to the sequestration of A $\beta$ 42 into amyloid plaques and indicate that MCI converters and AD patients are typically A $\beta$ +<sup>41</sup>. The A $\beta$ 34/

A $\beta$ 42 ratio is significantly elevated in the MCI converter and AD groups compared with the other groups (Fig. 6c).

To assess whether CSF-A $\beta$ 34 could provide important information during the early stages of AD, we tested whether A $\beta$ 34 could discriminate between MCI converters vs. non-converters from the Amsterdam Dementia Cohort. Receiver operating characteristic (ROC) curves of the CSF analytes were used to determine the accuracy of distinction between the MCI converters (i.e., prodromal AD) vs. stable patients. The area under the curve (AUC) for A $\beta$ 34 alone was slightly smaller than for A $\beta$ 42 (Fig. 6d). Interestingly, the A $\beta$ 34/A $\beta$ 42 ratio (AUC = 0.91) significantly improved the diagnostic accuracy compared with the classical A $\beta$ 40/A $\beta$ 42 ratio (AUC = 0.82) (Fig. 6e). An optimal cut-off analysis<sup>42</sup> yielded the best cut-off for an A $\beta$ 34/A $\beta$ 42 ratio >0.245, where sensitivity was 81.48% and specificity 82.35% (Supplementary Fig. 5d). The improved diagnostic accuracy of the A $\beta$ 34/A $\beta$ 42 ratio seemed specific for the distinction between MCI converters and stables. Similar AUCs ranging from 0.93 to 0.98 were obtained for A $\beta$ 42, A $\beta$ 40/A $\beta$ 42, and A $\beta$ 34/A $\beta$ 42 for the distinction between the SC and MCI converters or the SC and AD populations respectively (Supplementary Fig. 5e, f). For the distinction between MCI converters and stable patients, p-tau and t-tau yielded AUCs of 0.93 and 0.94, respectively (Fig. 6f). To assess how A $\beta$ 34/A $\beta$ 42 compares with the core AD biomarkers<sup>43</sup>, we calculated the ratio between the MCI converter and MCI stable groups (Fig. 6g). A $\beta$ 34/A $\beta$ 42 ranked third after the core markers, i.e., total- and phosphorylated-tau but before A $\beta$ 40/A $\beta$ 42 and A $\beta$ 42 (Fig. 6g). Overall, these results suggest that using A $\beta$ 34, an indicator for A $\beta$  degradation in combination with A $\beta$ 42, a core biomarker for A $\beta$  deposition, can improve the accuracy of prediction compared with A $\beta$ 40/A $\beta$ 42 regarding MCI patients who will convert to dementia vs. non-converters. The A $\beta$ 34/A $\beta$ 42 ratio could complement but not supplant existing biomarkers, such as CSF levels of total- and phosphorylated-tau. This finding suggests that, at certain stages of A $\beta$ 34 elevation in the CSF, the combination of this marker with reduced A $\beta$ 42 may indicate a failure in the clearance pathway associated with AD progression.

To test whether changes in the A $\beta$ 34/A $\beta$ 42 ratio are already detectable in earlier, pre-symptomatic AD, likely even before signs of neuronal injury become evident, we analyzed another 94 human CSF samples from cognitively normal, at-risk individuals from the PREVENT-AD cohort<sup>44</sup>. Individuals enrolled in this study have no diagnosable cognitive dysfunction and are in good general health, but they have a family history of a parent or multiple siblings affected with AD dementia<sup>45–47</sup>. At enrollment, these individuals were on average 10.2 years younger than the age of dementia onset for their earliest-affected relative. Consistent with our earlier Amsterdam Dementia Cohort findings, CSF-A $\beta$ 34 levels in the PREVENT-AD samples were not associated with age, *APOE*  $\epsilon$ 4, or gender (Supplementary Fig. 6a–c). We then tested whether an increased A $\beta$ 34/A $\beta$ 42 ratio (optimal cut-off A $\beta$ 34/A $\beta$ 42 > 0.245; Fig. 6e) could also be observed in cognitively normal individuals from the PREVENT-AD cohort. We identified 17 out of 94 individuals (18.09%) with A $\beta$ 34/A $\beta$ 42 ratios that were above our estimated cut-off.

According to current views, the asymptomatic phase of AD is characterized by a sequential appearance of abnormalities, starting with increased cortical A $\beta$  deposition (stage 1), leading to additional signs of neurodegeneration (stage 2; no abnormalities are seen in stage 0)<sup>48</sup>. Figure 7a depicts the A $\beta$ 42 and t-tau distribution of the PREVENT-AD samples from individuals at different stages of pre-symptomatic AD, with most individuals remaining in the stage 0 group. The horizontal and vertical dotted lines and shaded areas represent A $\beta$ 42<sup>41</sup> and t-tau cut-off values<sup>49,50</sup> and their inter-assay variances<sup>51</sup> (Fig. 7a). The biomarker assessments (validated CSF-A $\beta$ 42 cut-off values



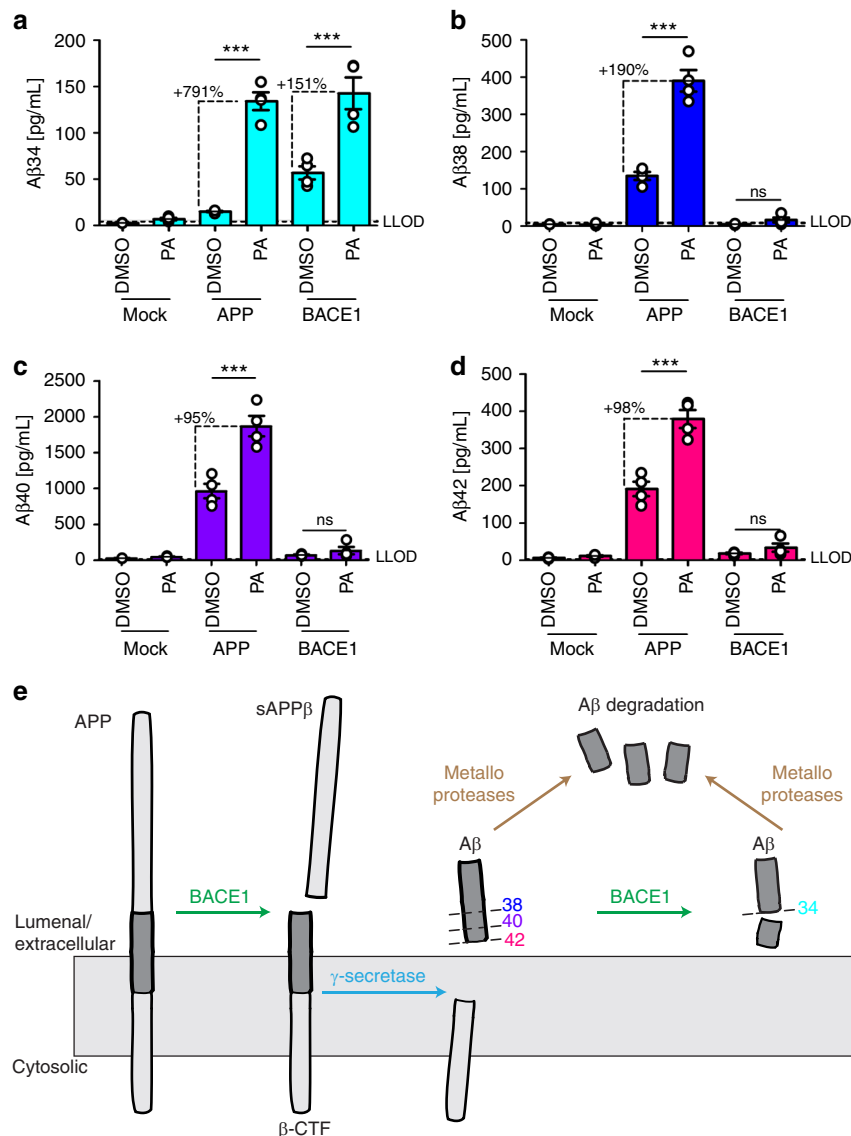


**Fig. 5** Aβ34 degradation by PA-sensitive metalloproteases. Using SH-SY5Y cells stably expressing APP695 or BACE1, MSD multiplexing to quantify the absolute amounts of Aβ34 (**a**), Aβ38 (**b**), Aβ40 (**c**), and Aβ42 (**d**) was performed. Data were collected from four independent experiments. Bars and error bars indicate mean ± s.e.m. Data were analyzed with two-way ANOVAs and significant interactions were followed up with simple main effects @treatment. \*\*\* $p < 0.001$ , ns = nonsignificant  $p > 0.05$ . **a** Aβ34, interaction  $F(2, 18) = 23.93$ ,  $p < 0.0001$ , simple main effects @Mock  $F(1, 18) = 0.12$ ,  $p > 0.05$ , @APP  $F(1, 18) = 97.02$ ,  $p < 0.0001$ , @BACE1  $F(1, 18) = 50.41$ ,  $p < 0.0001$ , **b** Aβ38, interaction  $F(2, 18) = 63.26$ ,  $p < 0.0001$ , simple main effects @Mock  $F(1, 18) = 0.002$ ,  $p > 0.05$ , @APP  $F(1, 18) = 197.54$ ,  $p < 0.0001$ , @BACE1  $F(1, 18) = 0.39$ ,  $p > 0.05$ , **c** Aβ40, interaction  $F(2, 18) = 25.54$ ,  $p < 0.0001$ , simple main effects @Mock  $F(1, 18) = 0.03$ ,  $p > 0.05$ , @APP  $F(1, 18) = 73.97$ ,  $p < 0.0001$ , @BACE1  $F(1, 18) = 0.34$ ,  $p > 0.05$ , **d** Aβ42, interaction  $F(2, 18) = 29.08$ ,  $p < 0.0001$ , simple main effects @Mock  $F(1, 18) = 0.07$ ,  $p > 0.05$ , @APP  $F(1, 18) = 97.47$ ,  $p < 0.0001$ , @BACE1  $F(1, 18) = 0.67$ ,  $p > 0.05$ . Schematic model (**e**) describes the proposed APP and Aβ processing pathways involving BACE1 and metalloproteases

including the inter-assay variances<sup>41,51</sup>) indicated that 15 PREVENT-AD participants are likely candidates having pre-clinical AD at stages 1 and 2 (Fig. 7a). Out of these, 11 presented with Aβ34/Aβ42 ratios above our cut-off ( $11/15 = 73.33\%$ ) (Fig. 7a). In addition, 6 out of 73 (8.22%) individuals at stage 0 also showed an elevated Aβ34/Aβ42 ratio. Individuals with elevated Aβ34/Aβ42 were not significantly older (Fig. 7b), but they exhibited significantly increased Cardiovascular Risk Factors, Aging, and Incidence of Dementia scores (CAIDE; Fig. 7c), and significantly increased CSF levels of total- and phosphorylated-tau (t-tau, p-tau; Fig. 7d, e).

**CSF-Aβ34 correlates with Aβ clearance in Aβ+ individuals.** In MCI and sporadic AD brain tissue, the levels and enzymatic

activity of BACE1 are increased<sup>9–11</sup> and localized to the surroundings of amyloid deposits<sup>12–15</sup>. Above, we presented evidence that Aβ34 (an amyloidolytic product of BACE1) is associated with BACE1-mediated Aβ clearance and is elevated in MCI converters, who show evidence of amyloid plaques (based on their CSF-Aβ42 levels<sup>41</sup>). Thus, we analyzed the CSF concentrations of Aβ34, Aβ38, Aβ40, and Aβ42 in Aβ+ and amyloid-negative (Aβ-) individuals (10 individuals per group; Fig. 8), whose Aβ turnover was previously assessed by SILK<sup>TM</sup><sup>31</sup>. SILK<sup>TM</sup> data of these 20 individuals were previously reported<sup>31</sup> and we correlated our results with the published data. The fractional turnover rate (FTR) or true fractional clearance rate<sup>31</sup>, which is associated with the irreversible loss of Aβ38, Aβ40, and Aβ42<sup>52</sup>, showed a significant positive correlation with the

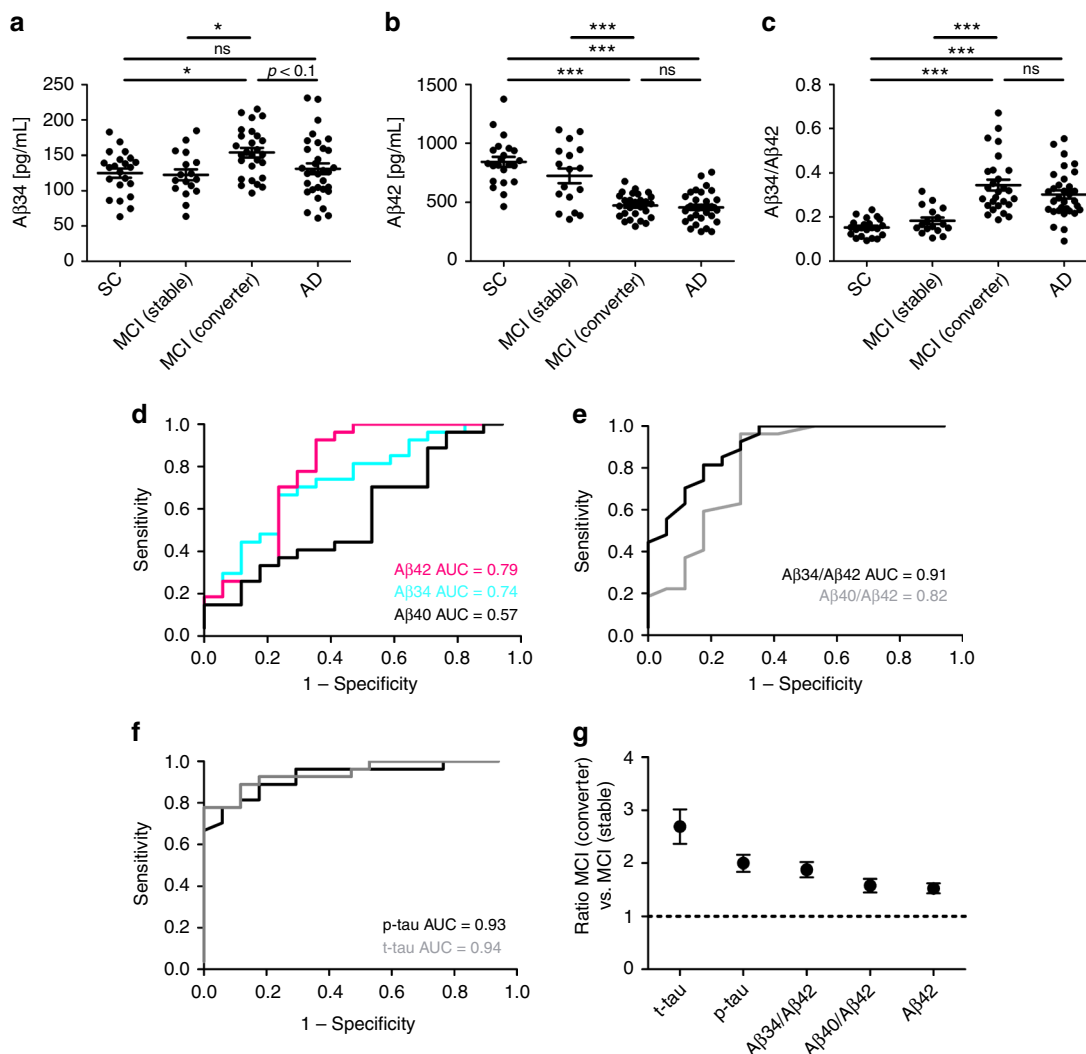


**Fig. 6** Aβ34 and core biomarkers in the Amsterdam Dementia Cohort. **a–c** Analyses of Aβ34 and Aβ42 in human CSF samples.  $n = 22$  subjective complaints (SC),  $n = 17$  MCI (stable),  $n = 27$  MCI (converter),  $n = 32$  Alzheimer’s disease (AD). Horizontal lines indicate mean  $\pm$  s.e.m. The data were analyzed with one-way ANOVAs and Tukey’s post-hoc tests (\*\*\* $p < 0.001$ , \* $p < 0.05$ , ns  $p > 0.05$ ). **a** Aβ34, one-way ANOVA  $F(3, 94) = 3.71$ ,  $p < 0.05$ , **b** Aβ42, one-way ANOVA  $F(3, 94) = 30.91$ ,  $p < 0.0001$ , **c** Aβ34/Aβ42, one-way ANOVA  $F(3, 94) = 21.71$ ,  $p < 0.0001$ . **d** Receiver operating characteristic (ROC) curves were computed on CSF levels of Aβ34, Aβ40, and Aβ42 in samples from the Amsterdam Dementia Cohort  $n = 17$  MCI (stable),  $n = 27$  MCI (converter). **e** ROC curves on Aβ40/Aβ42 and Aβ34/Aβ42 ratios from MCI (stable) and MCI (converter)). ROCs were compared using DeLong test: Aβ40/Aβ42 vs. Aβ34/Aβ42 ( $p = 0.0298$ ). **f** ROC curves on p-tau and t-tau from MCI (stable) and MCI (converter)). **g** Comparison of the performance of various molecules measured in CSF, which is based on average MCI (converter) to MCI (stable) ratios in the Amsterdam Dementia Cohort. The MCI (converter) to MCI (stable) ratio of Aβ42 was inverted for better comparison with the other ratios

CSF-Aβ34 concentrations only in Aβ+ individuals (Fig. 8a–c). Moreover, the CSF concentrations of Aβ38, Aβ40, and Aβ42 showed no significant correlation with Aβ38, Aβ40, or Aβ42 FTRs in our dataset (Fig. 8d–l). Interestingly, the ratio Aβ34/Aβ42 correlated with all three FTRs in Aβ– individuals, whereas the other ratios showed no correlation (Supplementary Fig. 7a–i). Overall, the correlation between Aβ34 and the clearance of the longer Aβ species is consistent with our results from rodent brains and SH-SY5Y cells, suggesting that elevated BACE1 levels in Aβ+ individuals might shift Aβ38, Aβ40, and Aβ42 into the Aβ34 degradation pathway. In conclusion, Aβ34 might serve as a surrogate marker for the overall clearance of Aβ38, Aβ40, and Aβ42 in Aβ+ and the ratio Aβ34/Aβ42 for the overall clearance in Aβ– individuals.

**Discussion**

In the AD field, research has traditionally focused on the conversion of APP into Aβ42 peptides leading to pathological amyloid plaque deposition in the brain and cognitive decline during the clinical progression of the disease. In recent years, however, emerging literature now identifies amyloid clearance as an important paradigm to better understand amyloid imbalances in sporadic AD patients.

BACE1 is thought to play a major role in the pathogenesis of AD and several inhibitors have been evaluated in clinical trials for their potential to slow or halt the production of neurotoxic Aβ peptides<sup>8</sup>. In order to attenuate disease progression in individuals with existing amyloid plaques, Aβ production would need to be inhibited by at least 95% since deposition is expected to be fast in

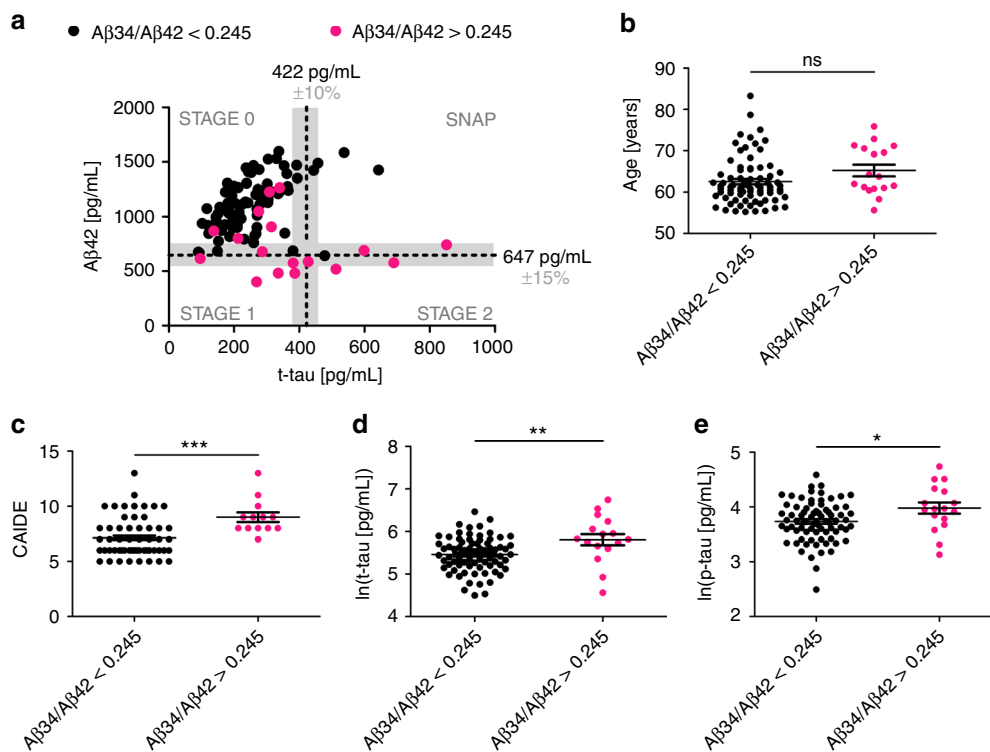


**Fig. 7** Aβ34, Aβ42, t-tau, and p-tau in PREVENT-AD. **a-e** PREVENT-AD Study: analysis of Aβ34, Aβ42, t-tau, and p-tau in CSF samples from cognitively normal individuals at risk for Alzheimer's disease ( $n = 94$ ). **a** Individuals can be separated into stages of pre-symptomatic AD, based on CSF biomarker assessment (t-tau cut-off > 422 pg/mL<sup>49,50</sup>, Aβ42 cut-off ≤ 647 pg/mL<sup>41</sup>, the gray shaded area indicates common inter-assay variances of the used cut-off values<sup>41,51</sup>). STAGE 0: t-tau and Aβ42 normal; STAGE1: t-tau normal and Aβ42 ≤ 647 pg/mL; STAGE 2: t-tau > 422 pg/mL, and Aβ42 ≤ 647 pg/mL; Suspected-non-AD pathology (SNAP): t-tau > 422 pg/mL and Aβ42 normal. Individuals with Aβ34/Aβ42 ratio above the optimal cut-off calculated in this study (Aβ34/Aβ42 > 0.245) are highlighted in magenta. **b-e** Comparison of age, Mann-Whitney  $U = 461.5$ ,  $p = 0.0586$  (**b**); Cardiovascular Risk Factors, Aging, and Incidence of Dementia (CAIDE), Mann-Whitney  $U = 184.5$ ,  $p = 0.0004$  (**c**); t-tau, unpaired  $t$ -test  $t(92) = 3.027$ ,  $p = 0.0032$  (**d**); and P<sub>181</sub>-tau (p-tau), unpaired  $t$ -test  $t(92) = 2.453$ ,  $p = 0.0168$  (**e**); between individuals with Aβ34/Aβ42 ratios above and below optimal cut-off (\*\*\* $p < 0.001$ , \*\* $p < 0.01$ , \* $p < 0.05$ , ns  $p > 0.05$ ). Horizontal lines indicate mean ± s.e.m.

Aβ+ individuals, even at lowered rates of newly produced Aβ<sup>53,54</sup>. Recently, current treatment approaches have been challenged based upon reports of disappointing results and adverse effects from BACE inhibitor trials (press release, 25 October 2018, Is there a role for BACE inhibition in Alzheimer's treatment?, Clinical Trials on Alzheimer's Disease (CTAD) conference).

BACE1 levels are increased in the AD brain<sup>9-11</sup>, and this could potentially result in increased Aβ production. However, a ~50% reduction in cerebral BACE1 (as reported in BACE1+/- mice and rats) does not alter Aβ38, Aβ40, and Aβ42 levels, suggesting that half the usual amount of BACE1 is sufficient to fully process endogenous APP<sup>32,33,35,36</sup>. Furthermore, increased enzyme levels do not lead to an increased amyloid load in the brains of mice overexpressing human BACE1<sup>55</sup>.

We found that cerebral Aβ34 levels were decreased by about 30% in BACE1+/- mice and by about 40% in wild-type rats, 1 h after intravenous injection of 1 mg/kg MK-8931 (with longer Aβ species unaltered). In the CSF of these MK-8931-treated rats, Aβ34 was the only Aβ species that was significantly decreased in the 1 and 20 mg/kg groups. However, since we administered the inhibitor intravenously, the greatest reduction in Aβ was likely achieved much earlier than in the original study, where rats received the compound orally and Aβ40 was significantly reduced in CSF and cortex at 1 and 3 h<sup>37</sup>. Due to the different routes of administration, our data cannot be directly compared with this study<sup>37</sup>. In contrast to the initial APP cleavage, BACE1 is a limiting factor for the amyloidolytic cleavage of longer Aβ species into Aβ34. Furthermore, our data imply that cerebral BACE1

possesses Aβ-degrading properties in vivo, as consistent with an earlier hypothesis based on in vitro studies<sup>19-21</sup>. The dichotomy between the amyloidogenic and amyloidolytic roles of BACE1 becomes more evident in experimental systems with elevated BACE1 levels. In the present study, for example, we found that an excess of APP favors amyloidogenic Aβ peptide production, but an excess of BACE1 results in increased Aβ degradation to Aβ34. Our characterization of the BACE1-mediated Aβ34 pathway is consistent with previous findings that cerebral BACE1 is not limiting for Aβ production<sup>32,33,35,36</sup>, observations that until now had remained unexplained due to our lack of understanding of amyloidolytic BACE1 activity.

As BACE1-derived Aβ34 can be further degraded by PA-sensitive metalloproteases<sup>21</sup>, it may be classified as a metastable intermediate in the degradation cascade of amyloidogenic peptides. The current findings show that this process is regulated by BACE1 expression such that when BACE1 may become limiting (i.e., when APP is overexpressed), amyloidogenic Aβ peptides are enzymatically degraded by both metalloproteases and BACE1. However, when BACE1 is present in sufficient or excess amounts (i.e., when overexpressed), the Aβ34 pathway is favored. As BACE1 is strongly expressed in neurons, particularly at sites of Aβ production in the brain<sup>14,15</sup>, longer Aβ peptides may be favorably converted into non-toxic Aβ34 at these sites. It is likely that Aβ34 might have a specific biological function and anti-apoptotic actions of this fragment on cultured human cells have been described<sup>21</sup>, however, a more thorough characterization is needed in order to determine its physiological role.

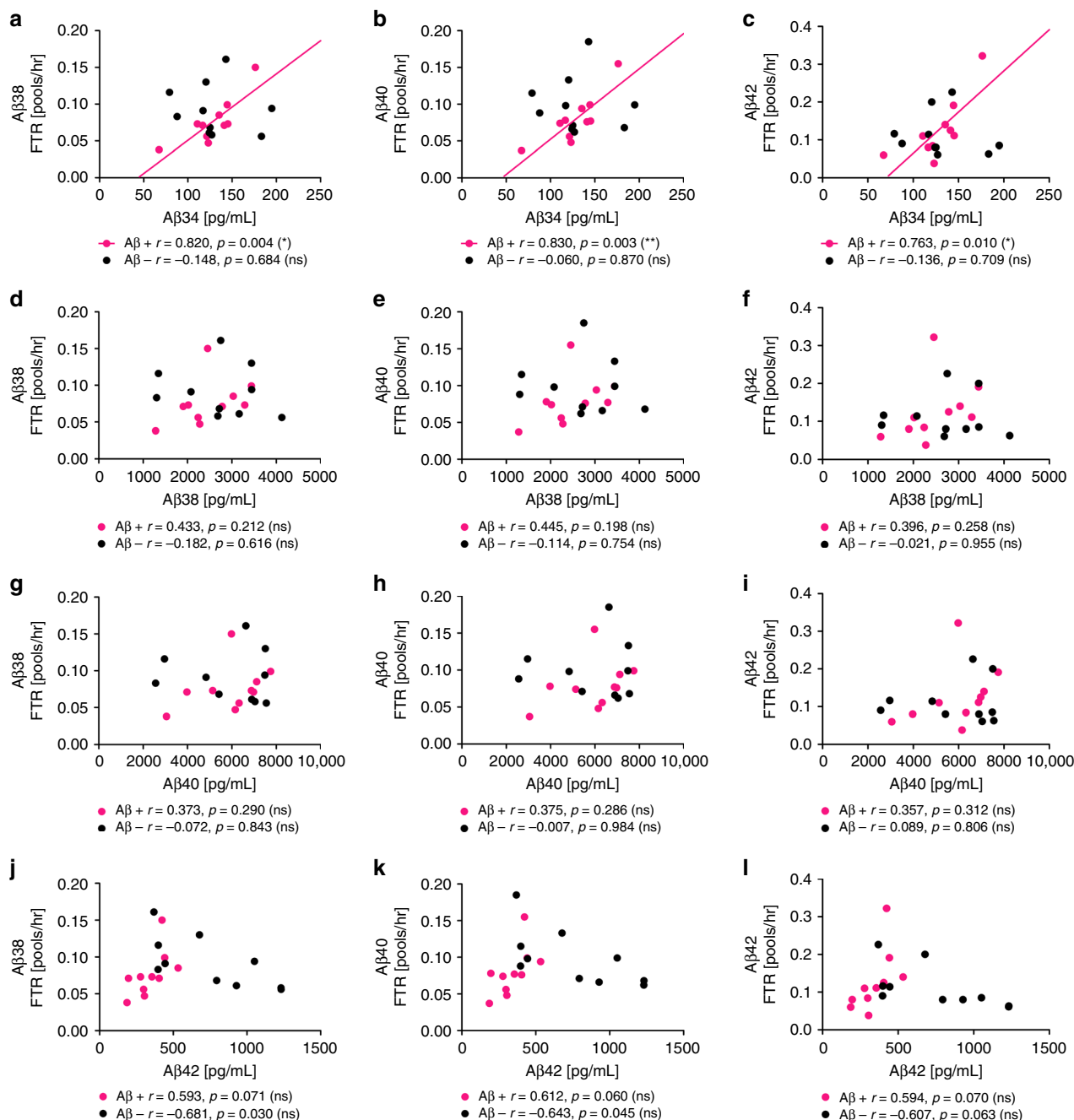


**Fig. 8** Association between CSF-A $\beta_{34}$  and A $\beta$  clearance rates. Analysis of A $\beta_{34}$ , A $\beta_{38}$ , A $\beta_{40}$ , and A $\beta_{42}$  in human CSF with ultra-sensitive assays (Meso Scale Discovery (MSD)). A $\beta_{38}$ , A $\beta_{40}$ , and A $\beta_{42}$  clearance (fractional turnover rate, FTR) was previously measured using stable isotope labeling kinetic (SILK)<sup>31</sup>. Samples were from  $n = 10$  A $\beta^+$  and  $n = 10$  A $\beta^-$  individuals. Scatterplots of CSF-A $\beta_{34}$  (**a-c**), A $\beta_{38}$  (**d-f**), A $\beta_{40}$  (**g-i**), or A $\beta_{42}$  (**j-l**) with A $\beta_{38}$  FTR (**a, d, g, j**), A $\beta_{40}$  FTR (**b, e, h, k**), or A $\beta_{42}$  FTR (**c, f, i, l**). Pearson correlation coefficients ( $r$ ) were computed to assess the relationship between the variables. The Bonferroni adjusted  $p$ -values are: \*\* $p < 0.003$ , \* $p < 0.016$ , ns = nonsignificant  $p > 0.0125$

Site-specific mutations in APP were found in rare cases of familial early-onset AD (FEOAD) and processing at the  $\beta$ -cleavage site of APP could be causally linked to increased and decreased risk of AD. For example,  $\beta$ -cleavage of APP carrying the Swedish mutation (KM670/671NL) is increased and causes FEOAD<sup>56</sup>. In contrast, the Icelandic mutation (A673T) protects against AD<sup>57</sup>, primarily by reducing the  $\beta$ -cleavage of APP, as well as modulating A $\beta$  aggregation<sup>58</sup>. In light of our findings, it is plausible that the Icelandic mutation results in reduced A $\beta$  generation, whereas BACE1-mediated A $\beta$  degradation still occurs. Although inhibition of BACE1-mediated cleavage of APP

remains an attractive therapeutic approach in AD, it appears that reducing BACE1-mediated generation of pathogenic A $\beta$  peptides alone will not be sufficient to stop plaque growth<sup>53,54</sup>. Furthermore, BACE1 inhibition is likely to affect amyloidolytic cleavage of longer A $\beta$  species into smaller, non-amyloidogenic A $\beta_{34}$ . For this reason, we tested for clearance effects in human CSF and, notably, we found elevated baseline levels of A $\beta_{34}$  in MCI patients who later progressed to AD. A $\beta_{34}$  can be detected in human plasma samples<sup>59</sup>, therefore, it would be interesting to test whether its levels in CSF and plasma correlate or whether MCI converters show elevated amounts of plasma-A $\beta_{34}$ . By combining

an indicator for A $\beta$  degradation (i.e., A $\beta$ 34) and a biomarker for A $\beta$  deposition (i.e., A $\beta$ 42), we found that the A $\beta$ 34/A $\beta$ 42 ratio significantly improved the diagnostic accuracy to distinguish between prodromal AD and stable MCI compared with the classical A $\beta$ 40/A $\beta$ 42 ratio. However, elevated CSF levels of p-tau and t-tau showed the best distinction between the two MCI groups. An elevated A $\beta$ 34/A $\beta$ 42 ratio in the prodromal stage of AD could indicate that, at early stages of A $\beta$  plaque formation (i.e., decreased CSF-A $\beta$ 42 levels<sup>41</sup>), the increased levels and amyloidolytic activity of BACE1 elicit a defense reaction (i.e., increased generation of A $\beta$ 34 to facilitate amyloid clearance). Although BACE1 levels are elevated around fibrillar A $\beta$ <sup>12–15</sup>, the fibrillar conformation is resistant to BACE1 cleavage because of its unique structure<sup>60</sup> (under the condition of their co-presence in a cellular compartment with a low pH). A $\beta$ 42 fibrils are stabilized by hydrophobic clusters in such a way that they do not grant BACE1 access to the A $\beta$ 34 cleavage site<sup>60</sup>. Furthermore, since only A $\beta$ 42 turnover (and not A $\beta$ 38 or A $\beta$ 40) is altered when amyloidosis has started<sup>31</sup>, the surplus of A $\beta$ 34 could be mainly derived from A $\beta$ 42 since its conformation is different from A $\beta$ 38 and A $\beta$ 40. We speculate that intracellular A $\beta$ 42 can adopt a conformation that is favorable for fibril formation, which makes it especially susceptible to BACE1-mediated degradation at the A $\beta$ 34 cleavage site.

We hypothesized that the A $\beta$ 34/A $\beta$ 42 ratio might be potentially useful to monitor pre-symptomatic AD, as changes in the classical biomarkers of AD pathogenesis can already be observed before cognitive symptoms appear<sup>48</sup>. In human samples from the PREVENT-AD cohort (i.e., at-risk individuals without current cognitive impairment), we found that the A $\beta$ 34/A $\beta$ 42 ratio was elevated, especially in individuals whose biomarker assessment classified them in stages 1 and 2 (signs of cortical A $\beta$  deposition). Overall, few individuals in PREVENT-AD showed reduced CSF-A $\beta$ 42 ( $\leq 647$  pg/mL<sup>41</sup>). In families with autosomal-dominant AD, reduced CSF-A $\beta$ 42 and increased tau in asymptomatic mutation carriers were already detected 10–20 years before the estimated age of onset<sup>61</sup>. At present, members of the PREVENT-AD cohort tend to be several years younger compared with the onset of dementia in their affected relative(s) and, in contrast to mutation carriers, they probably vary substantially in their degree of progression of pre-symptomatic AD. Interestingly, we identified individuals in stage 0 with an elevated A $\beta$ 34/A $\beta$ 42 ratio. However, our data are cross-sectional and should not be interpreted as representing change over chronological ageing. Therefore, it will be crucial to follow the longitudinal trajectory of A $\beta$ 34 in these individuals, in combination with classical CSF measures, since we expect that these biomarker changes are closely related to aging, as previously seen in cognitively normal middle-aged volunteers<sup>62</sup>.

Consistent with the concept of amyloid clearance and deposition mechanisms indicating failed clearance in pre-symptomatic stages of AD, we find that the A $\beta$ 34 levels in CSF correlate with the overall clearance rates of A $\beta$ 38, A $\beta$ 40, and A $\beta$ 42 in A $\beta$ + but not A $\beta$ - individuals. In contrast, the CSF A $\beta$ 34/A $\beta$ 42 ratios correlate with the overall clearance rates of A $\beta$ 38, A $\beta$ 40, and A $\beta$ 42 in A $\beta$ - but not A $\beta$ + individuals. Since inter-individual variances in A $\beta$  clearance rates are affected by various factors including age, genetics, or pathological processes<sup>24,31,52,63</sup>, it is rather unlikely that the levels of an individual protein, such as BACE1, could determine the overall A $\beta$  clearance from the brain. However, our findings suggest that under pathological conditions, elevated BACE1 levels in the brain direct a large proportion of A $\beta$ 38, A $\beta$ 40, and A $\beta$ 42 into BACE1-mediated A $\beta$  clearance via the A $\beta$ 34 degradation pathway. Given this, A $\beta$ 34 might be used as a marker for the overall clearance of these peptides in A $\beta$ + individuals. We speculate that under non-pathological conditions,

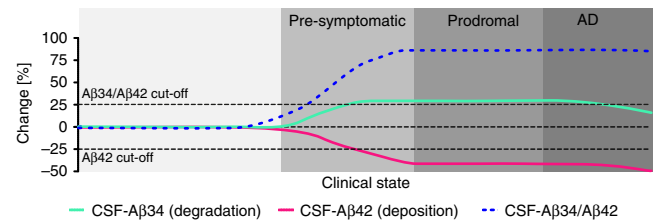


**Fig. 9** Conceptual model of early changes in AD. Before a clinical diagnosis of Alzheimer's disease (AD), decades of A $\beta$  peptide deposition lead to plaque formation in pre-symptomatic and prodromal stages of the disease. Incorporating A $\beta$ 34 (marker of enzymatic A $\beta$  degradation) with measures of A $\beta$ 42 (marker for cerebral A $\beta$  deposition) could complement current biomarker assessments and provide additional information about A $\beta$  turnover

a special relationship exists between A $\beta$ 34 and A $\beta$ 42, which might explain the correlation of their ratio with the overall A $\beta$  clearance. Once A $\beta$ 42 gets deposited in plaques, the correlation with clearance is lost, likely due to an altered A $\beta$ 42 degradation. Under these circumstances, A $\beta$ 34 alone becomes the predictor of clearance rates.

In summary, our results show that, *in vivo*, BACE1 is limiting for the degradation of longer A $\beta$  peptides into the intermediate A $\beta$ 34. The levels of this amyloidolytic fragment are elevated in the CSF of prodromal AD patients (i.e., MCI that progresses to AD). Thus, incorporating A $\beta$ 34 as a marker of amyloid clearance with a marker of amyloid deposition (i.e., A $\beta$ 42) might complement current CSF measures, especially in clinical intervention trials that aim at a modulation of APP processing (Fig. 9). Ultimately, the present study proposes that enzymatic processes affecting A $\beta$  metabolism are altered in early phases of AD and, accordingly, A $\beta$ 34 can be used to monitor A $\beta$  turnover at earlier stages of this devastating disease.

## Methods

**Synthetic A $\beta$  peptides.** Synthetic peptides A $\beta$ 34, A $\beta$ 35, A $\beta$ 38, A $\beta$ 40, and A $\beta$ 42 (PSL, Germany) dissolved in formic acid and vacuum dried in a speed-vac (Thermo) were resuspended (2 mg/mL) in 1% Milli-Q/ammonia water, ultrasonicated (10 min 4 °C), diluted to 1 mg/mL with Milli-Q and ultrasonicated again. Peptide concentrations ( $\epsilon = 1490$  M/cm), integrity, and molecular weight were confirmed by absorption measurements at 280 nm (Synergy H1, BioTek Instruments Inc. plate reader), Coomassie dye stains after performing denaturing polyacrylamide gel electrophoresis (SDS-PAGE), and matrix-assisted laser desorption ionization mass spectrometry (Bruker UltrafleXtreme MALDI-TOF/TOF system in standard reflector-positive mode; samples mixed 1:1 with  $\alpha$ -cyanocinnamic acid matrix and applied to ground steel targets using dried-droplet method).

**BACE1-mediated A $\beta$  degradation *in vitro*.** BACE1 from Fc purification<sup>64</sup> 10  $\mu$ g/mL (a kind gift from Johan Lundkvist, AstraZeneca) was incubated with synthetic A $\beta$ 35, A $\beta$ 40, or A $\beta$ 42 at 50  $\mu$ g/mL for 10 min at 37 °C in 20 mM (sodium acetate/HCl, pH4.5), directly mixed 1:1 with  $\alpha$ -cyanocinnamic acid matrix, and applied to ground steel targets using dried-droplet method.

**MSD assay.** Using the ELISA Conversion Kit from MSD (USA), an electrochemiluminescence-based assay was developed (neo-epitope specific A $\beta$ 34 and the sulfo-tagged 6E10 (binds to the N-terminus of human A $\beta$ ) or the sulfo-tagged 4G8 for rodent samples (binds to the mid domain of A $\beta$ )). High-bind or custom-printed 4-plex plates (using our mab34, 4G8 (Biolegend) for pan-A $\beta$  assay, G2-10 for 1-plex A $\beta$ 40 assay, and MSD's validated mouse monoclonal anti-A $\beta$ 38, anti-A $\beta$ 40, as well as anti-A $\beta$ 42 antibodies, see MSD A $\beta$  peptide V-PLEX) were blocked (MSD 5% Blocker A in PBS) for 1 h at 22 °C and washed three times with PBS-Tween (PBS-T) for 1 min at 22 °C, loaded with SULFO-TAG<sup>TM</sup> 6E10 or 4G8 detection antibody (diluted to 1 $\times$  in MSD Diluent 100) and sample or peptide calibrator (in MSD Diluent 35 or cell culture medium), and incubated for 16 h at 4 °C with shaking at 600 rpm. After three washing steps with PBS-T for 1 min at 22 °C, 150  $\mu$ L 2 $\times$  MSD read buffer was added per well. All plates were read using an MSD QuickPlex SQ 120 Imager and data analyzed using MSD Workbench<sup>®</sup> software. Standard curves were fitted using a non-linear four-parameter logistic fit



with  $1/y^2$  weighting. The equation is:

$$y = b_2 + \frac{b_1 - b_2}{1 + \left(\frac{x}{b_3}\right)^{b_4}} \quad (1)$$

$y$  = signal,  $x$  = concentration,  $b_2$  = estimated response at infinite concentration,  $b_1$  = estimated response at Zero concentration,  $b_3$  = mid-range concentration,  $b_4$  = slope factor.

In the WORKBENCH® software, lower limit of detection (LLOD) was determined as the analyte concentration equivalent to the signal that is  $2.5 \times$  standard deviations (SD) above the back-fit signal of the blank. Assay performance (inter-plate, intra-plate coefficient of variation (CV), LLOD, and upper limit of detection (ULOD)) were assessed using peptide calibrators in MSD diluent 35 (Supplementary Fig. 1e). Spike-and-recovery and linearity-of-dilution assessments for human CSF samples (compared with calibrators in MSD diluent 35) are given in Supplementary Table 1.

**Western blot analysis.** Lithium dodecyl sulfate loading buffer (Invitrogen) with 2-Mercaptoethanol (final concentration 5% (v/v)) was added to samples and the mix was heated to 70 °C for 10 min. Proteins were separated on 4–12% bis/tris gradient gels. Novex® Sharp Pre-Stained Protein Standard (Invitrogen) was used. Peptides/proteins were transferred onto polyvinylidene fluoride membranes (Millipore) by tank blotting (Bio-Rad) at 4 °C. The primary antibodies, anti-actin C4 dilution 1:4000 (Millipore, Catalog #MAB1501), anti-APP ectodomain 22C11 dilution 1:10,000 (Millipore, Catalog #MAB348), anti-BACE1 D10E5 dilution 1:2000 (Cell Signaling, Catalog #mAb5606), anti-sAPP $\beta$  dilution 1:2000 (IBL, Catalog #IP18957), and secondary antibodies dilutions 1:10,000 (horseradish peroxidase-conjugated anti-mouse, anti-rabbit, Promega, Catalog #W4021 and # W4011), were used. Most important full-size western blots are displayed in Supplementary Fig. 8. Signals were recorded on ImageQuant LAS 500 or Amersham Imager 600 (GE Healthcare Life Sciences).

**Mouse brain lysates.** We complied with all relevant ethical regulations for animal testing and research. Brains were obtained from BACE1 $-/-$  and BACE1 $+/-$  mice, as well as their wild-type littermates<sup>65</sup> in accordance with the guidelines of the Institutional Animal Care and Use Committee at the University of Kiel. Frozen mouse brains were thawed on ice, weighed and homogenized in 100 mM Tris-HCl, 150 mM NaCl, 2 $\times$  complete protease inhibitor cocktail (Roche) using gentle-MACS™ M Tubes/Dissociator at 4 °C (Miltenyi Biotech). Triton X-100 was added for a final concentration of 1% and brain homogenates were lysed for 1 h at 4 °C. Lysates were centrifuged at  $10,621 \times g$  in a microfuge (Eppendorf) at 4 °C for 15 min to remove nuclear fraction. Samples were diluted in the appropriate buffers for protein determination using bicinchoninic acid assay (BCA assay, Pierce) and MSD assays.

**Pharmacological treatment of rats.** We complied with all relevant ethical regulations for animal testing and research. Experiments were approved by the McGill Animal Care Ethics Committee. Six to 8 weeks old male Sprague–Dawley rats were housed at the Douglas Mental Health University Institute animal facility and treatments were performed in accordance with the guidelines of the Canadian Council on Animal Care. Rats were intravenously injected with indicated concentrations of MK-8931 (Selleckchem) or vehicle (20% Cyclodextrin) and samples were collected after 1 h of treatment. CSF was collected with the aid of a stereotaxic instrument to appropriately position the head of the rat and samples stored at  $-80$  °C. Brain tissue samples were harvested and immediately preserved on dry ice, later stored at  $-80$  °C. Rat brain lysates were prepared in the same way as mouse brain lysates.

**Plasmids, mutagenesis.** Human full-length BACE1 (isoform A) and human full-length APP (isoform APP695, with an N-terminal Myc tag and a C-terminal FLAG tag), in the mammalian expression vector pCEP4, Hygro (Invitrogen) were used for expression. All constructs were verified by DNA sequencing.

**Cell culture and transfection.** Human neuroblastoma (SH-SY5Y) cells (DSMZ No.: ACC 209; DSMZ, Braunschweig, Germany) were cultured in 50% Dulbecco's modified Eagle's medium, 50% Hams-F12, 10% fetal bovine serum, 2 mM L-glutamine, 0.5 mM sodium pyruvate, 1 $\times$  MEM non-essential amino-acid solution in a humidified incubator at 37 °C with 5% CO<sub>2</sub>. Cells were routinely tested for mycoplasma contamination. SH-SY5Y cells were transfected using TransFectin™ according to the manufacturer's instructions (Bio-Rad) and stable clones were selected using 250  $\mu$ g/mL Hygromycin B. For experiments, culturing medium without Hygromycin B was used and conditioned for 16 h. Protease inhibitors, were dissolved in Dimethyl sulfoxide (DMSO) at a 1000 $\times$  concentration and compared with vehicle treatment (DMSO 1:1000). Cells were harvested on ice. Cell culture supernatants were collected, centrifuged for 10 min at  $450 \times g$  in a micro-centrifuge at 4 °C and used for further analysis. Cells were washed once on ice with ice-cold PBS<sup>++</sup> and lysed in 20 mM Tris-HCl, pH 7.5, 150 mM NaCl, 20 mM 3-[(3-cholamidopropyl) dimethyl-ammonio]-1-propanesulfonate (CHAPS), 2 $\times$  Complete protease inhibitor (Roche), for 60 min at 4 °C. Cell lysates were

centrifuged for 15 min at  $10,621 \times g$  in a microcentrifuge at 4 °C to remove nuclear fraction.

**CSF samples.** We complied with all relevant ethical regulations for work with human participants. The studies were performed in accordance with The Code of Ethics of the World Medical Association (Declaration of Helsinki). The studies were approved by the regional ethics committees. Written informed consent was received from participants prior to inclusion in the studies.

CSF samples for initial assay development were received from the Clinic at the Division of Psychiatry, Zurich. CSF samples from individuals with SILK data<sup>31</sup> were obtained from the Department of Neurology, Washington University in St. Louis. CSF samples from individuals with different clinical diagnoses were received from the Amsterdam Dementia Cohort and the time interval between CSF collection and assessment of cognition was <24 h<sup>66</sup>. CSF samples from cognitively normal individuals at risk for AD (PREVENT-AD study) were received from the Douglas Mental Health University Institute and the time interval between CSF collection and assessment of cognition was on average  $5.6 \pm 3.9$  (SD) months<sup>44</sup>. The experimentalist was blinded from diagnosis until completion of measurements. Diagnoses of probable AD<sup>67</sup> or MCI<sup>68</sup>, were made by consensus of a multidisciplinary team according to diagnostic criteria. For the Amsterdam Dementia Cohort, patients who presented with cognitive complaints but were considered as normal after thorough investigation (i.e., criteria for MCI, dementia or any psychiatric or neurological results not fulfilled) were defined as patients with subjective cognitive complaints (SC). Subjects were followed annually and MCI to AD conversion (or MCI that remained stable) was defined based on conversion to AD within 3 years after the CSF collection, and stable as no conversion occurred within 3 years. Lumbar punctures after an overnight fast were performed using the Sprotte 24-gauge atraumatic needle. Samples were aliquoted into propylene cryotubes and stored at  $-80$  °C. Procedures from the BIOMARK-APD consortium of the EU Joint Program in Neurodegenerative Disease were used for sample preparation and measurements<sup>69</sup>. A summary of samples included in the study is given in Supplementary Table 2. CSF t-tau, p-tau, and A $\beta$ 42 were measured using INNOTEST ELISA; Fujirebio (formerly Innogenetics).

**Statistical analysis.** The statistical evaluation was carried out by GraphPad Prism, SPSS, MedCalc Version 18.2.1, and the indicated statistical tests and algorithms (analysis of variance (ANOVA),  $t$ -test, Pearson correlation, Mann–Whitney  $U$ -tests, Spearman correlations, De Long statistics to compare ROC curves<sup>70</sup>). The optimal cut-off (point on the ROC curve with the minimum distance ( $d$ ) to sensitivity = 1 and specificity = 1)<sup>42</sup> was determined using Pythagoras' theorem:

$$d = \sqrt{(1 - \text{sensitivity})^2 + (1 - \text{specificity})^2} \quad (2)$$

Individual data points, mean and s.e.m. are displayed in the figures. Data were tested for normality, using violation of the Shapiro–Wilk test at  $p < 0.01$  as the criterion. Data sets not meeting the normality assumption were analyzed using non-parametric tests (as indicated in the figure legends).

**Reporting summary.** Further information on research design is available in the Nature Research Reporting Summary linked to this article.

## Data availability

Data used in the preparation of this article were obtained from the Pre-symptomatic Evaluation of Novel or Experimental Treatments for Alzheimer's Disease (PREVENT-AD) program (<http://www.prevent-alzheimer.ca>) data release 2.0 (30 November 2015, Update: 07 June 2016). Other relevant data are available directly from the authors.

Received: 1 May 2018 Accepted: 17 April 2019

Published online: 20 May 2019

## References

- Hardy, J. & Selkoe, D. J. The amyloid hypothesis of Alzheimer's disease: progress and problems on the road to therapeutics. *Science* **297**, 353–356 (2002).
- Walsh, D. M. & Selkoe, D. J. Oligomers on the brain: the emerging role of soluble protein aggregates in neurodegeneration. *Protein Pept. Lett.* **11**, 213–228 (2004).
- Wilquet, V. & De Strooper, B. Amyloid-beta precursor protein processing in neurodegeneration. *Curr. Opin. Neurobiol.* **14**, 582–588 (2004).
- Thinakaran, G. & Koo, E. H. Amyloid precursor protein trafficking, processing, and function. *J. Biol. Chem.* **283**, 29615–29619 (2008).
- Takami, M. et al. gamma-Secretase: successive tripeptide and tetrapeptide release from the transmembrane domain of beta-carboxyl terminal fragment. *J. Neurosci.* **29**, 13042–13052 (2009).

6. Olsson, F. et al. Characterization of intermediate steps in amyloid beta (Abeta) production under near-native conditions. *J. Biol. Chem.* **289**, 1540–1550 (2014).
7. Glabe, C. G. & Kaye, R. Common structure and toxic function of amyloid oligomers implies a common mechanism of pathogenesis. *Neurology* **66**, S74–S78 (2006).
8. Mullard, A. BACE inhibitor bust in Alzheimer trial. *Nat. Rev. Drug Discov.* **16**, 155 (2017).
9. Fukumoto, H., Cheung, B. S., Hyman, B. T. & Irizarry, M. C. Beta-secretase protein and activity are increased in the neocortex in Alzheimer disease. *Arch. Neurol.* **59**, 1381–1389 (2002).
10. Holsinger, R. M., McLean, C. A., Beyreuther, K., Masters, C. L. & Evin, G. Increased expression of the amyloid precursor beta-secretase in Alzheimer's disease. *Ann. Neurol.* **51**, 783–786 (2002).
11. Yang, L. B. et al. Elevated beta-secretase expression and enzymatic activity detected in sporadic Alzheimer disease. *Nat. Med.* **9**, 3–4 (2003).
12. Sadleir, K. R., Eimer, W. A., Kaufman, R. J., Osten, P. & Vassar, R. Genetic inhibition of phosphorylation of the translation initiation factor eIF2alpha does not block Abeta-dependent elevation of BACE1 and APP levels or reduce amyloid pathology in a mouse model of Alzheimer's disease. *PLoS ONE* **9**, e101643 (2014).
13. Sadleir, K. R. et al. Presynaptic dystrophic neurites surrounding amyloid plaques are sites of microtubule disruption, BACE1 elevation, and increased Abeta generation in Alzheimer's disease. *Acta Neuropathol.* **132**, 235–256 (2016).
14. Zhao, J. et al. Beta-site amyloid precursor protein cleaving enzyme 1 levels become elevated in neurons around amyloid plaques: implications for Alzheimer's disease pathogenesis. *J. Neurosci.* **27**, 3639–3649 (2007).
15. Kandalepas, P. C. et al. The Alzheimer's beta-secretase BACE1 localizes to normal presynaptic terminals and to dystrophic presynaptic terminals surrounding amyloid plaques. *Acta Neuropathol.* **126**, 329–352 (2013).
16. Zhang, X. M. et al. Beta-secretase-1 elevation in transgenic mouse models of Alzheimer's disease is associated with synaptic/axonal pathology and amyloidogenesis: implications for neuritic plaque development. *Eur. J. Neurosci.* **30**, 2271–2283 (2009).
17. Kimura, A., Hata, S. & Suzuki, T. Alternative selection of beta-site APP-cleaving enzyme 1 (BACE1) cleavage sites in amyloid beta-protein precursor (APP) harboring protective and pathogenic mutations within the Abeta sequence. *J. Biol. Chem.* **291**, 24041–24053 (2016).
18. Hernandez-Guillamon, M. et al. Sequential amyloid-beta degradation by the matrix metalloproteases MMP-2 and MMP-9. *J. Biol. Chem.* **290**, 15078–15091 (2015).
19. Fluhrer, R. et al. Identification of a beta-secretase activity, which truncates amyloid beta-peptide after its presenilin-dependent generation. *J. Biol. Chem.* **278**, 5531–5538 (2003).
20. Shi, X. P. et al. Beta-secretase cleavage at amino acid residue 34 in the amyloid beta peptide is dependent upon gamma-secretase activity. *J. Biol. Chem.* **278**, 21286–21294 (2003).
21. Caillava, C. et al. Study on Abeta34 biology and detection in transgenic mice brains. *Neurobiol. Aging* **35**, 1570–1581 (2014).
22. Portelius, E. et al. beta-site amyloid precursor protein-cleaving enzyme 1 (BACE1) inhibitor treatment induces Abeta5-X peptides through alternative amyloid precursor protein cleavage. *Alzheimer's Res. Ther.* **6**, 75 (2014).
23. Mattsson, N. et al. BACE1 inhibition induces a specific cerebrospinal fluid beta-amyloid pattern that identifies drug effects in the central nervous system. *PLoS ONE* **7**, e31084 (2012).
24. Mawuenyega, K. G. et al. Decreased clearance of CNS beta-amyloid in Alzheimer's disease. *Science* **330**, 1774 (2010).
25. Iliff, J. J. et al. A paravascular pathway facilitates CSF flow through the brain parenchyma and the clearance of interstitial solutes, including amyloid beta. *Sci. Transl. Med.* **4**, 147ra111 (2012).
26. Deane, R., Sagare, A. & Zlokovic, B. V. The role of the cell surface LRP and soluble LRP in blood-brain barrier Abeta clearance in Alzheimer's disease. *Curr. Pharm. Des.* **14**, 1601–1605 (2008).
27. Lewczuk, P. et al. The amyloid-beta (Abeta) peptide pattern in cerebrospinal fluid in Alzheimer's disease: evidence of a novel carboxyterminally elongated Abeta peptide. *Rapid Commun. Mass Spectrom.* **17**, 1291–1296 (2003).
28. Saido, T. & Leissring, M. A. Proteolytic degradation of amyloid beta-protein. *Cold Spring Harb. Perspect. Med.* **2**, a006379 (2012).
29. Portelius, E. et al. Ex vivo (18)O-labeling mass spectrometry identifies a peripheral amyloid beta clearance pathway. *Mol. Neurodegener.* **12**, 18 (2017).
30. Bateman, R. J. et al. Human amyloid-beta synthesis and clearance rates as measured in cerebrospinal fluid in vivo. *Nat. Med.* **12**, 856–861 (2006).
31. Patterson, B. W. et al. Age and amyloid effects on human central nervous system amyloid-beta kinetics. *Ann. Neurol.* **78**, 439–453 (2015).
32. Weber, M. et al. BACE1 across species: a comparison of the in vivo consequences of BACE1 deletion in mice and rats. *Sci. Rep.* **7**, 44249 (2017).
33. Rabe, S. et al. The Swedish APP mutation alters the effect of genetically reduced BACE1 expression on the APP processing. *J. Neurochem.* **119**, 231–239 (2011).
34. Sala Frigerio, C. et al. Beta-secretase cleavage is not required for generation of the intracellular C-terminal domain of the amyloid precursor family of proteins. *FEBS J.* **277**, 1503–1518 (2010).
35. Nishitomi, K. et al. BACE1 inhibition reduces endogenous Abeta and alters APP processing in wild-type mice. *J. Neurochem.* **99**, 1555–1563 (2006).
36. Georgievskaya, B. et al. Revisiting the peripheral sink hypothesis: inhibiting BACE1 activity in the periphery does not alter beta-amyloid levels in the CNS. *J. Neurochem.* **132**, 477–486 (2015).
37. Kennedy, M. E. et al. The BACE1 inhibitor verubecestat (MK-8931) reduces CNS beta-amyloid in animal models and in Alzheimer's disease patients. *Sci. Transl. Med.* **8**, 363ra150 (2016).
38. Sadleir, K. R., Eimer, W. A., Cole, S. L. & Vassar, R. Abeta reduction in BACE1 heterozygous null 5XFAD mice is associated with transgenic APP level. *Mol. Neurodegener.* **10**, 1 (2015).
39. König, G., Masters, C. L. & Beyreuther, K. Retinoic acid induced differentiated neuroblastoma cells show increased expression of the beta A4 amyloid gene of Alzheimer's disease and an altered splicing pattern. *FEBS Lett.* **269**, 305–310 (1990).
40. Belyaev, N. D. et al. The transcriptionally active amyloid precursor protein (APP) intracellular domain is preferentially produced from the 695 isoform of APP in a {beta}-secretase-dependent pathway. *J. Biol. Chem.* **285**, 41443–41454 (2010).
41. Palmqvist, S. et al. Accuracy of brain amyloid detection in clinical practice using cerebrospinal fluid beta-amyloid 42: a cross-validation study against amyloid positron emission tomography. *JAMA Neurol.* **71**, 1282–1289 (2014).
42. Indrayan, A. *Medical Biostatistics* 3rd edn, (CRC Press, Boca Raton, FL, 2013).
43. Olsson, B. et al. CSF and blood biomarkers for the diagnosis of Alzheimer's disease: a systematic review and meta-analysis. *Lancet Neurol.* **15**, 673–684 (2016).
44. Breitner, J. C. S., Poirier, J., Etienne, P. E. & Leoutsakos J.M. Rationale and Structure for a New Center for Studies on Prevention of Alzheimer's Disease (StoP-AD). *J. Prev. Alzheimer's Dis.* **3**, 236–242 (2016).
45. van Duijn, C. M. et al. Familial aggregation of Alzheimer's disease and related disorders: a collaborative re-analysis of case-control studies. *Int. J. Epidemiol.* **20**(Suppl 2), S13–S20 (1991).
46. Cupples, L. A. et al. Estimating risk curves for first-degree relatives of patients with Alzheimer's disease: the REVEL study. *Genet. Med.* **6**, 192–196 (2004).
47. Fratiglioni, L., Ahlbom, A., Viitanen, M. & Winblad, B. Risk factors for late-onset Alzheimer's disease: a population-based, case-control study. *Ann. Neurol.* **33**, 258–266 (1993).
48. Jack, C. R. Jr. et al. An operational approach to National Institute on Aging-Alzheimer's Association criteria for preclinical Alzheimer disease. *Ann. Neurol.* **71**, 765–775 (2012).
49. Le Bastard, N. et al. Comparison of two analytical platforms for the clinical qualification of Alzheimer's disease biomarkers in pathologically-confirmed dementia. *J. Alzheimer's Dis.* **33**, 117–131 (2013).
50. Struyfs, H., Molinuevo, J. L., Martin, J. J., De Deyn, P. P. & Engelborghs, S. Validation of the AD-CSF-index in autopsy-confirmed Alzheimer's disease patients and healthy controls. *J. Alzheimer's Dis.* **41**, 903–909 (2014).
51. Mattsson, N. et al. CSF biomarker variability in the Alzheimer's Association quality control program. *Alzheimer's Dement. J. Alzheimer's Assoc.* **9**, 251–261 (2013).
52. Elbert, D. L., Patterson, B. W. & Bateman, R. J. Analysis of a compartmental model of amyloid beta production, irreversible loss and exchange in humans. *Math. Biosci.* **261**, 48–61 (2015).
53. Wolfe, M. S. *The Molecular and Cellular Basis of Neurodegenerative Diseases: Underlying Mechanisms*. (Elsevier Science & Technology Books, Amsterdam, The Netherlands, 2018).
54. Roberts, B. R. et al. Biochemically-defined pools of amyloid-beta in sporadic Alzheimer's disease: correlation with amyloid PET. *Brain* **140**, 1486–1498 (2017).
55. Lee, E. B. et al. BACE overexpression alters the subcellular processing of APP and inhibits Abeta deposition in vivo. *J. Cell Biol.* **168**, 291–302 (2005).
56. Haass, C. et al. The Swedish mutation causes early-onset Alzheimer's disease by beta-secretase cleavage within the secretory pathway. *Nat. Med.* **1**, 1291–1296 (1995).
57. Jonsson, T. et al. A mutation in APP protects against Alzheimer's disease and age-related cognitive decline. *Nature* **488**, 96–99 (2012).
58. Benilova, I. et al. The Alzheimer disease protective mutation A2T modulates kinetic and thermodynamic properties of amyloid-beta (Abeta) aggregation. *J. Biol. Chem.* **289**, 30977–30989 (2014).
59. Pannee, J. et al. The amyloid-beta degradation pattern in plasma—a possible tool for clinical trials in Alzheimer's disease. *Neurosci. Lett.* **573**, 7–12 (2014).
60. Gremer, L. et al. Fibril structure of amyloid-beta(1-42) by cryo-electron microscopy. *Science* **358**, 116–119 (2017).
61. Fagan, A. M. et al. Longitudinal change in CSF biomarkers in autosomal-dominant Alzheimer's disease. *Sci. Transl. Med.* **6**, 226ra230 (2014).

62. Sutphen, C. L. et al. Longitudinal cerebrospinal fluid biomarker changes in preclinical Alzheimer disease during middle age. *JAMA Neurol.* **72**, 1029–1042 (2015).
63. Potter, R. et al. Increased in vivo amyloid-beta42 production, exchange, and loss in presenilin mutation carriers. *Sci. Transl. Med.* **5**, 189ra177 (2013).
64. Bridges, K. G. et al. A novel approach to identifying beta-secretase inhibitors: bis-statine peptide mimetics discovered using structure and spot synthesis. *Peptides* **27**, 1877–1885 (2006).
65. Dominguez, D. et al. Phenotypic and biochemical analyses of BACE1- and BACE2-deficient mice. *J. Biol. Chem.* **280**, 30797–30806 (2005).
66. van der Flier, W. M. et al. Optimizing patient care and research: the Amsterdam Dementia Cohort. *J. Alzheimer's Dis.* **41**, 313–327 (2014).
67. McKhann, G. et al. Clinical diagnosis of Alzheimer's disease: report of the NINCDS-ADRDA Work Group under the auspices of Department of Health and Human Services Task Force on Alzheimer's Disease. *Neurology* **34**, 939–944 (1984).
68. Petersen, R. C. et al. Mild cognitive impairment: clinical characterization and outcome. *Arch. Neurol.* **56**, 303–308 (1999).
69. Del Campo, M. et al. Facilitating the validation of novel protein biomarkers for dementia: an optimal workflow for the development of sandwich immunoassays. *Front Neurol.* **6**, 202 (2015).
70. DeLong, E. R., DeLong, D. M. & Clarke-Pearson, D. L. Comparing the areas under two or more correlated receiver operating characteristic curves: a nonparametric approach. *Biometrics* **44**, 837–845 (1988).

## Acknowledgements

Thanks to Robert Umek and Martin Boissonneault (Meso Scale Discovery) for their help and support with the electrochemiluminescence assay development, to Konrad Beyreuther and Chris Weise for discussions, as well as Peter Kang and Arturo Aliaga for technical support with the rat experiments. We thank Johan Lundkvist for providing us with Fc-BACE1 and discussions. We thank the PREVENT-AD group (public-private partnership using funds provided by McGill University, the Fonds de Recherche du Québec – Santé (FRQ-S), an unrestricted research grant from Pfizer Canada, the Levésque Foundation, the Douglas Hospital Research Centre and Foundation, the Government of Canada, and the Canada Fund for Innovation). The Founding Director of the program is John C. S. Breitner, MD, MPH, Douglas Hospital Research Centre and Faculty of Medicine, McGill University, Montréal, QC, Canada. Program Co-Directors include Associate Directors Judes Poirier, PhD, and Pierre Etienne, MD, and Deputy Director Pedro Rosa-Neto, MD, PhD, all at the same institutions. For up-to-date information, see <http://www.preventalzheimer.ca>. Thanks to Brain@McGill, the Velux Stiftung, the Natural Sciences and Engineering Research Council of Canada, the Canadian Consortium on Neurodegeneration in Aging, and the Canadian Institute of Health Research (MOP-133411) for support awarded to G.M., C.H., L.K., or F.L. Thanks to the Studienstiftung des Deutschen Volkes, and the Groupe de Recherche Axé

sur la Structure des Protéines (GRASP, McGill University) for Ph.D. fellowships awarded to F.L., and the DFG (SFB877-TPA3) for funding awarded to P.S. G.M. holds both a Canada Research Chair in Molecular Pharmacology and a Canada Foundation for Innovation (CFI) grant. The McGill SPR-MS Facility thanks the CFI for infrastructure support.

## Author contributions

F.L. designed and performed experiments, analyzed data, prepared the figures, and wrote the manuscript. L.K., A.S., I.U., M.A.H., V.E. and P.K. designed and performed experiments, analyzed data, and helped writing the manuscript. C.T., W.M.v.d.F., P. R.-N., Ph. S., J.P., P.S., R.J.B., J.B., and C.H. designed experiments, analyzed data, and helped writing the manuscript. G.M. conceived the study, designed experiments, analyzed data, and wrote the manuscript. All authors have approved the final version of the manuscript.

## Additional information

**Supplementary Information** accompanies this paper at <https://doi.org/10.1038/s41467-019-10152-w>.

**Competing interests:** The authors declare no competing interests.

**Reprints and permission** information is available online at <http://npg.nature.com/reprintsandpermissions/>

**Journal peer review information:** *Nature Communications* thanks Dominic Walsh and other anonymous reviewer(s) for their contribution to the peer review of this work.

**Publisher's note:** Springer Nature remains neutral with regard to jurisdictional claims in published maps and institutional affiliations.



**Open Access** This article is licensed under a Creative Commons Attribution 4.0 International License, which permits use, sharing, adaptation, distribution and reproduction in any medium or format, as long as you give appropriate credit to the original author(s) and the source, provide a link to the Creative Commons license, and indicate if changes were made. The images or other third party material in this article are included in the article's Creative Commons license, unless indicated otherwise in a credit line to the material. If material is not included in the article's Creative Commons license and your intended use is not permitted by statutory regulation or exceeds the permitted use, you will need to obtain permission directly from the copyright holder. To view a copy of this license, visit <http://creativecommons.org/licenses/by/4.0/>.

© The Author(s) 2019